HEPL-170
16K/Gen-2

AN EXPERIMENT ON THE LIMITS OF QUANTUM ELECTRODYNAMICS

W. C. Barber, Burton Richter, and W. K. H. Panofsky,
Stanford University,

and

G. K. O'Neill and B. Gittelman,
Princeton University

Internal Report
Not to be Published

June 1959

Supported by the joint program of the Office of Naval Research
and the U. S. Atomic Energy Commission under
Contract N6onr-25116 (NR 022 026).

High-Energy Physics Laboratory
W. W. Hansen Laboratories of Physics
Stanford University
Stanford, California

DISCLAIMER

CONTENTS

		Page
I.	LIMITATIONS OF ELECTRODYNAMIC CUTOFF EXPERIMENTS	1
II.	OUTLINE OF EXPERIMENT	6
III.	OUTLINE OF EXPERIMENTAL PROBLEMS	12
IV.	TIME SCHEDULE AND COOPERATIVE ARRANGEMENTS	16
V.	TABLE OF PARAMETERS	19

Appendix

A.	DELAY LINE INFLECTOR	21
B.	MAGNET CELL STRUCTURE	27
C.	CAPTURE EFFICIENCY	30
D.	RADIATION DAMPING TIMES AND BEAM SIZE	32
E.	BEAM LOSS RATE DUE TO QUANTUM FLUCTUATIONS	37
F.	LOSSES DUE TO SCATTERING AND BREMSSTRAHLUNG	40
G.	INTERACTION REGION STABILITY	44
H.	CROSS SECTIONS, COUNTING RATES, AND BACKGROUND	48
I.	VACUUM SYSTEM AND TRAPPED-ION BEAM INSTABILITIES	60
J.	RADIOFREQUENCY POWER	64
REFERENCES		65

I. LIMITATIONS OF ELECTRODYNAMIC CUTOFF EXPERIMENTS*

Quantum electrodynamics (QED), the most modern description of the interaction of charges with the electromagnetic field, was developed in the late 1940's. By the end of that period, the theory based on suggestions of Kramers and Bethe, and worked on by Tomonaga, Feynman, Dyson, Schwinger, and others, was shown to agree closely with experiments. The energy level shift in hydrogen, measured by Lamb and Retherford, was found to be a sensitive test of the higher-order radiative corrections of QED. To summarize, among the interactions known in modern physics the interaction of charges with the electromagnetic field is at present the best understood. Because we have at present no proof that our understanding of QED extends to the critically important size range below a nucleon radius, the question of limits of validity of QED is of great interest. That such limits might exist at high values of momentum transfer has frequently been proposed. Although QED has succeeded in describing the basic known phenomena quantitatively and completely, this success has been achieved by a systematic method of subtracting divergent integrals. Although such integrals are eliminated from present theory, one cannot ignore the fact that physical facts may eventually be found that will make such integrals finite. This experiment is aimed at uncovering evidence bearing on this point.

Experiments on the charge distributions of the neutron and proton, the magnetic moment of the muon, the Lamb shift, and the magnetic form

---

*This report is a revision of O'Neill, Barber, Richter, and Panofsky, "A proposed experiment on the limits of quantum electrodynamics," Stanford University High-Energy Physics Laboratory proposal, May 1958 (unpublished), and a description of the present plans.

factor of the proton, have placed limits on the validity of QED. Specifically, each of these experiments can be interpreted to yield a lower bound on distance and an upper bound on momentum transfer within which the theoretical basis of the interpretation must be valid.

The experiments on nucleon structure as carried out by elastic and inelastic electron scattering have yielded quantitative data on nucleon radii if the validity of QED is assumed; in these experiments a breakdown of QED is fundamentally indistinguishable from the effects of nucleon structure. Hence independent study of the limits of QED is necessary to the interpretation of high-energy electron-scattering experiments on nucleons in terms of nucleon structure alone. The experiments of Hofstadter and collaborators[1] have given an apparent rms radius of 0.8×10^{-13} cm for the proton, and a much smaller number (~ 0 within errors) for the corresponding charge radius of the neutron. Although we cannot untangle possible electrodynamics breakdown from these observations, we can interpret the radius of 0.8×10^{-13} cm as an upper limit at which deviations might occur. (We will make this statement more quantitative below.)

Feynman and Speisman[2] suggested that the neutron-proton mass difference ($\sim 2.53\ m_e$) could be explained by a small-distance (high-energy) cutoff on electrodynamics. Or, if one compares the proton size limit from the mass difference ($< 0.4 \times 10^{-13}$ cm) with the radius measured by electron scattering, the discrepancy could be explained by a cutoff at 0.3×10^{-13} cm on electrodynamics.

Recently Heisenberg has suggested a theory of elementary particles based on the idea of a fundamental length of $\sim 10^{-13}$ cm. He has tried to calculate several of the natural constants by assuming such a spatial structure. Several other attempts to introduce a fundamental length of this order have been made by various authors in the past, none with quantitative success.

There is at present no experimental evidence whatever that discrepancies with QED exist; the remarks above simply indicate possible limits beyond those presently explored. Before describing a unique experimental method that should greatly extend these limits or determine a deviation,

this section will summarize the limitations of other electrodynamic cutoff experiments so far performed or suggested.* In general, experiments on a possible short-distance alteration of electrodynamics must involve either high energy or extreme accuracy.

The experiments in question do not all necessarily place limits on the same fundamental quantity. It can be shown by relativistic invariance requirements that a deviation is most likely to depend on the invariant momentum transfer $q^2 = (\Delta\vec{q})^2 - (\Delta E)^2$, where $\Delta\vec{q}$ is the three-dimensional momentum transfer and ΔE the energy transfer. For light particles such as the electron at high energies or for real photons, this number is always essentially zero; hence deviations will occur in terms of cutting off the amplitude of virtual photons or electrons at high values of q. There is no known reason (although there could be an overriding principle) why the cutoff on electron or photon momenta should occur at the same value; hence both of these cutoffs should be investigated experimentally.

The experiments in question are listed below, (A)-(F):

(A) Electron-electron scattering. This is in principle the most nearly definitive electrodynamics experiment, involving only electrons and photons. The lowest-order diagram is Fig. I-1, in which p_1 and p_2 are the electron momenta, and q is the momentum transferred by the photon. In the center-of-mass ("c.m.") system, the amplitude of the virtual photon (the "photon propagator") is the Fourier transform of the Coulomb potential $1/r$. If we replace $1/r$ by $(1/r)(1 - e^{-\Lambda r})$, the corresponding alteration of the propagator would reduce the Møller scattering cross section by the factor $1 + (2q^2/\hbar^2\Lambda^2)$. In an experiment with a stationary target electron and an incident electron of energy E_0, $q_{c.m.} < (2m_0E_0)^{\frac{1}{2}}$,

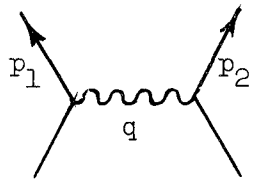

FIG. I-1. Lowest-order Feynman diagram for electron-electron scattering.

*The remainder of this section is based mainly on a lecture by S. D. Drell and on subsequent conversations with him. For a more detailed treatment, see reference 4.

where m_0 is the rest mass of the electron; so $q_{c.m.} < E_0^{\frac{1}{2}}$, with q and E_0 in Mev. A 10% experiment at 8-Bev laboratory energy could just detect a cutoff length $1/\Lambda = 0.5 \times 10^{-13}$ cm. In order to probe to a distance (defined as Λ^{-1}) small compared with a nucleon radius--say, 1/6 of 0.7×10^{-13} cm--we would require a 10% experiment at 1000 Bev.

(b) Electron-proton scattering. In this experiment, carried out by Hofstadter and collaborators, the first-order diagram is similar to that of Møller scattering (Fig. I-2). However, the mass of the proton lowers the c.m. velocity, and allows q to be much higher for a given E_0. If we make the same modification to the virtual photon propagator as before, Hofstadter's results can be written

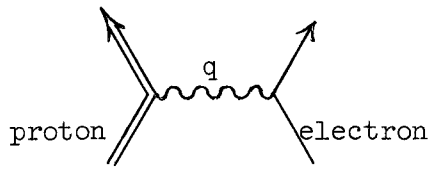

FIG. I-2. Lowest-order Feynman diagram for electron-proton scattering.

$$\langle r^2 \rangle_{measured} = \langle r^2 \rangle_{proton} + (6/\Lambda^2) = (0.8 \times 10^{-13} \text{ cm})^2 .$$

Even if we assume the "true" charge radius of the proton to be zero, this experiment limits Λ^{-1} to $[\langle r^2 \rangle_{measured}/6]^{\frac{1}{2}} < 0.33 \times 10^{-13}$ cm. If we guess $[\langle r^2 \rangle_{proton}]^{\frac{1}{2}} \sim 0.4 \times 10^{-13}$ cm, Λ^{-1} would be 0.29×10^{-13} cm. As a measure of an upper limit on a cutoff for electrodynamics, Hofstadter's experiment is therefore equivalent to e-e scattering at about 20 Bev.

(C) Lamb shift. The agreement of existing theory with experiment on the 1057-Mc splitting between the $2S_{\frac{1}{2}}$ and $2P_{\frac{1}{2}}$ levels in hydrogen is now within 0.2 Mc. An apparent proton size of 0.8×10^{-13} cm would cause an 0.12-Mc shift in the 2S level, so the Lamb-Retherford experiment limits Λ^{-1} to 0.5×10^{-13} cm or less.

(D) Ground state energy level in hydrogen. The diagram for this is the same as for e-p scattering, and the same questions of interpretation arise in both experiments.

(E) Anomalous magnetic moment of the muon. Berestetskii, Krokhin, and Khlebnilov[3] have worked out an order-of-magnitude result. The factor

is

$$1 + \frac{\alpha}{2\pi}\left[1 - \frac{2}{3}\frac{1}{(\lambda\!\!\!^{-}_{C}\,\Lambda)^2}\right] ,$$

where $\lambda\!\!\!^{-}_{C}$ is the muon Compton wavelength (2×10^{-13} cm) and $\alpha/2\pi$ is the Schwinger correction to the moment. A 2% measurement of the already small anomalous part of the magnetic moment would be required even to equal the 0.33×10^{-13} cm limit set by e-p scattering. In case a discrepancy was to be found in such an experiment, the question of interpretation would arise, due to possible unknown structure in the muon.

(F) Large-angle pair production in hydrogen. Two such experiments, the first of which has been carried out by Richter at Stanford,[4] have been discussed in detail by Drell.[5] Their potential limits appear to be 0.7 and 0.3×10^{-13} cm, respectively (the present experimental limits are larger); each relates to a possible alteration of a virtual electron propagator. As discussed above, at present no necessary connection is known between electron- and photon-propagator breakdown experiments.

In this summary of experiments, there are several with limits of $\Lambda^{-1} \sim 0.3$ to 0.5×10^{-13} cm [$(\langle r^2 \rangle_{QED})^{\frac{1}{2}} \sim 0.7$ to 1.2×10^{-13} cm]. If we design a new experiment for the purpose of testing QED, we must be sure that a positive identification of a deviation can be made, down to deviations smaller than the limits discussed above. We would like to see a deviation of ~40% in a 10% experiment in order to be reasonably confident that a deviation, if any, was real. If we require that our experiment show a 40% deviation for $(\langle r^2 \rangle_{QED})^{\frac{1}{2}} = 0.25 \times 10^{-13}$ cm or be able to set limits of $(\langle r^2 \rangle_{QED})^{\frac{1}{2}} = 1.2 \times 10^{-14}$ cm if no deviation is observed, we must perform the equivalent of a 1000-Bev e-e scattering experiment. In the next section, a design for such an experiment will be described. Actually, it is hoped to obtain a statistical accuracy of much better than 10%, probably of the order of 1%.

II. OUTLINE OF THE EXPERIMENT

One of the most direct measurements possible on quantum electrodynamics is almost certainly electron-electron scattering. To improve present limits by an order of magnitude, and to check the question of the neutron-proton mass difference, one should have about 1 Bev available in the c.m. system. By conventional methods it would require a 1000-Bev accelerator to achieve such a c.m. energy, so it is natural to turn to beam-on-beam techniques.

The possibility of carrying out a high-energy e-e scattering experiment by colliding beams in storage rings was considered in 1956.[6,7] Shortly afterward, V. A. Petukhov[8] suggested performing the experiment with a FFAG accelerator very similar to a type later proposed by Ohkawa of the MURA group.[9]

In the course of work done at Princeton during late 1956, it became obvious that the scattering experiment would be relatively easy with storage rings if a high-intensity linear accelerator could be used as a source. In January 1957, Ball began calculating the initial parameters for such an experiment.[10] Fortunately, an unpublished report by Christy[11] appeared in time to relieve Ball of the most difficult calculation he intended to make. The favorable results obtained by Ball for estimated damping times, counting rates, and beam lifetime, prompted the continuation of the calculations on a full-time basis during the Summer of 1957 by P. Federbush. In that period, after a check of Ball's results, the interaction region forces were studied and estimates of the most important background effects were made. The efficiency for continuous capture of electrons initially injected at an equilibrium radius larger than that defined by the r-f was also calculated. In September 1957

a new type of pulsed magnetic deflector design was worked out;[12] it was studied by V. Korenman and its construction in full scale was begun.

Discussions with the group at the Stanford University High-Energy Physics Laboratory were begun in April 1957; not until later in the year was it felt that the calculations justified an actual proposal. A formal request for support of this experiment was made in June 1958, funds were granted by the joint program of the Office of Naval Research and the U.S. Atomic Energy Commission as an amendment to the High-Energy Physics Laboratory master contract N6onr-25116, and detailed design and construction of apparatus was begun upon the receipt of support in January 1959. The testing of completed apparatus is expected to begin early in 1960 (see IV, below).

We are preparing to carry out the experiment at several energies between 100 and 500 Mev, using a pair of storage rings and the Stanford Mark III linear accelerator (Figs. II-1 and II-2). The storage rings, of 1.42-meter radius with a total weight of 45 tons, will enclose a stainless-steel vacuum chamber capable of reaching very high vacua. A radiofrequency cavity will be provided in each storage ring to make up radiation losses. The feasibility of this proposal depends on the strong damping of betatron and synchrotron oscillations that occurs as a result of the classical synchrotron radiation. This damping, with a characteristic time of about 10 milliseconds at 500 Mev, will produce stable circulating currents of a density which is not limited by Liouville's theorem as in the case of undamped orbits. The damping permits the injection system to be designed for the continuous addition of new accelerator pulses to make up for losses. The radiation damping will also reduce the loss rate due to multiple gas scattering to a negligibly small value. Only one important effect leading to a loss of electrons appears to exist: the quantum fluctuation spread in the synchrotron radiation. By choice of a sufficiently small r-f phase angle, even this loss can be kept very small. Although the experiment can be carried out successfully with a storage time of as little as two minutes, we are designing for storage times of about a day, to allow for errors of calculation in this unfamiliar field.

Only one novel piece of apparatus is needed in this experiment: the inflector to transfer accelerator pulses to the storage rings. Our present

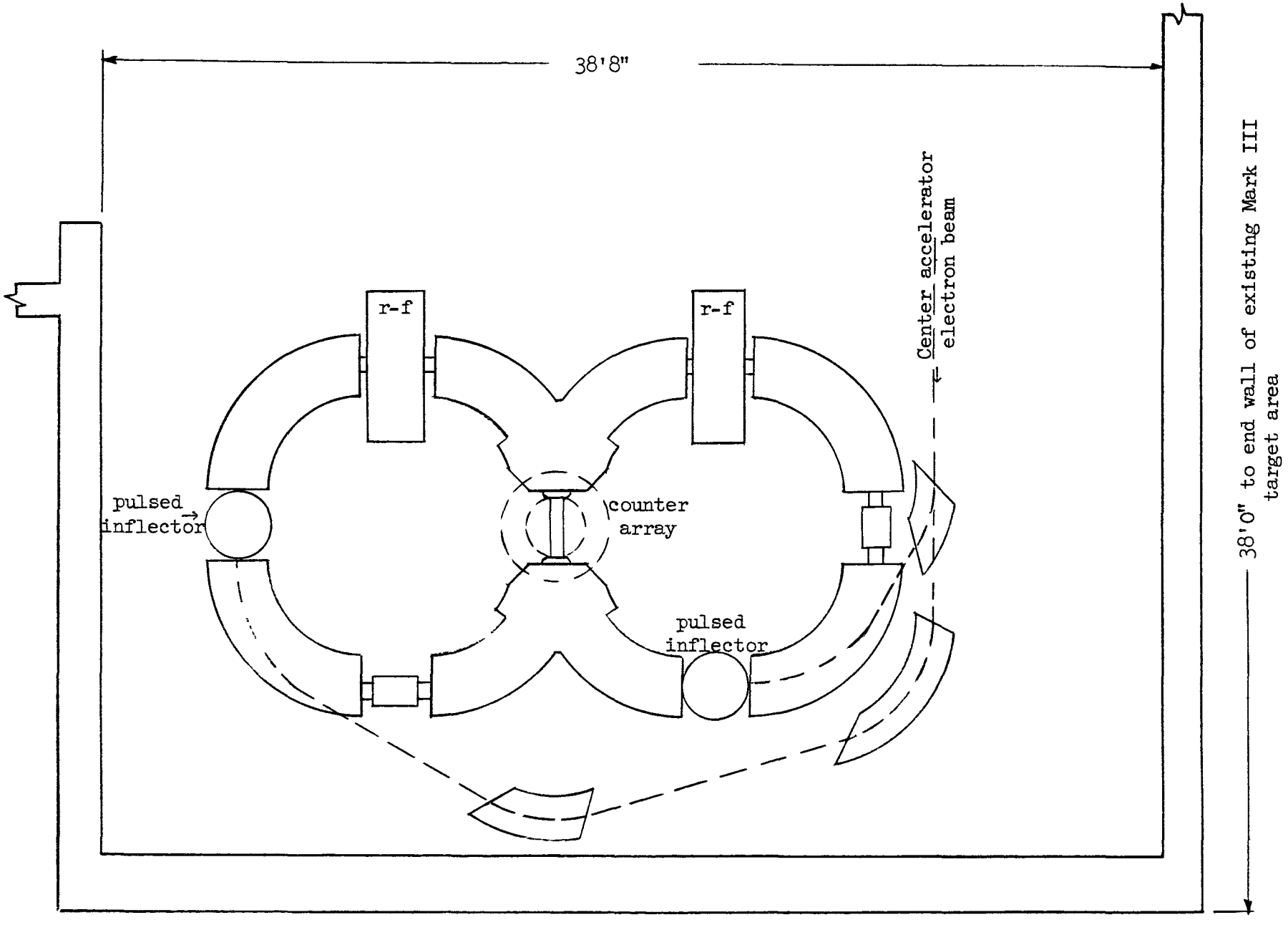

FIG. II-1.-- Floor plan of new experimental area showing location of storage rings and injecting magnets.

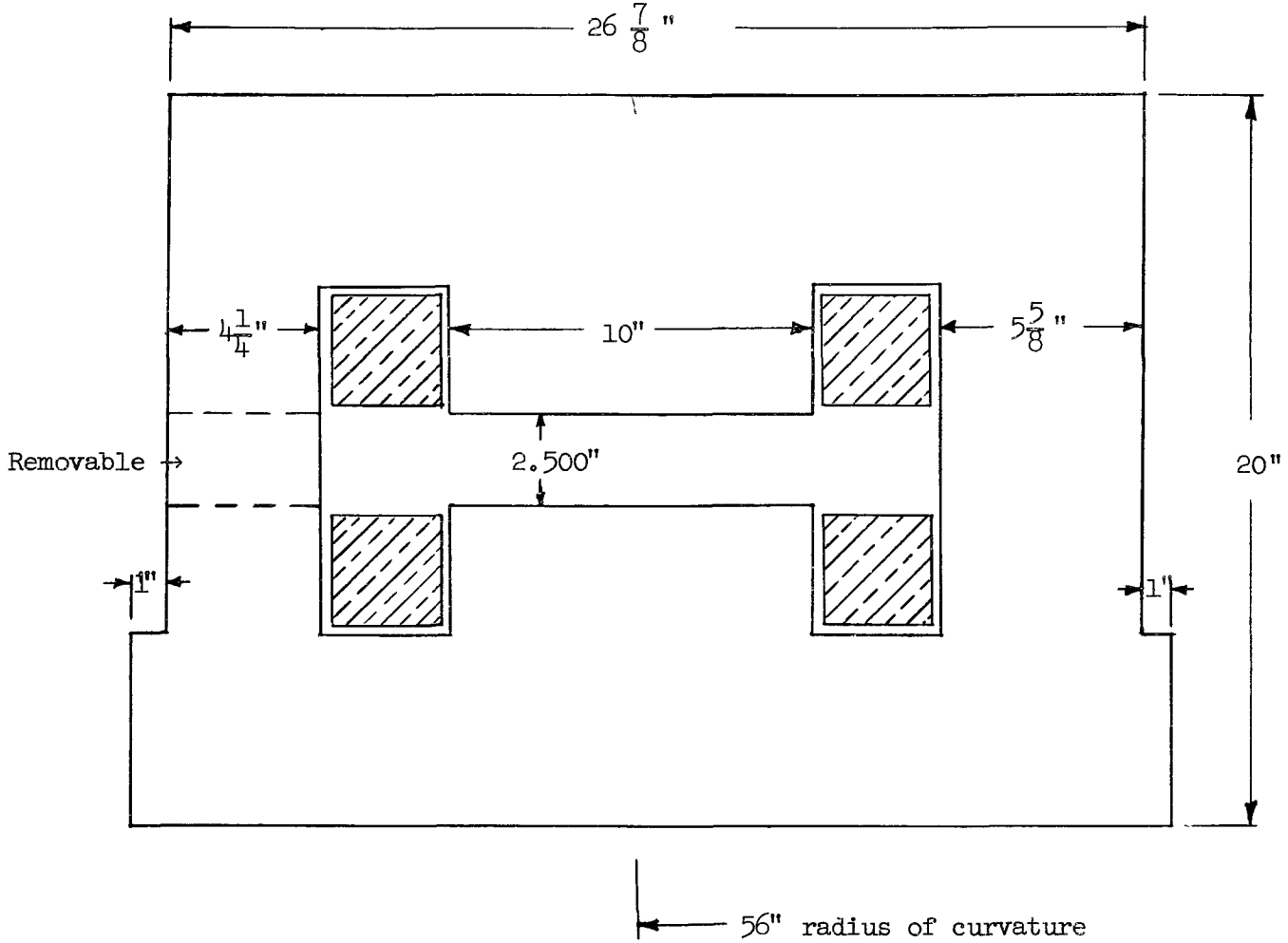

FIG. II-2.-- Cross section of storage-ring magnets

design for this device is being checked by its construction in full scale; the necessary equipment has been procured and testing is now going on. Since the efficiency of transfer affects only the buildup time, not the final beam size or beam current, the requirements on the inflector are not strict, and no serious difficulty is expected with this device.

It appears that the electron beams will form flat ribbons of charge, about 5-mm wide and possibly no more than 100-μ high. By the addition of small steering magnets, the beams will be made to cross at a small angle. This will prevent instabilities due to the interaction-region forces, will make the counting rates independent of beam thickness, and will localize the source volume to a few centimeters in longest dimension. Observation will be made by a large cluster of counters in coincidence pairs, subtending a solid angle of about a sixth of a sphere. At the design value of 1-amp circulating current, the total counting rate should be about 3 counts/sec, with an excellent true/background ratio. The experiment should still be possible if, for unforeseen reasons, currents of no more than 100 ma can be achieved. Our counter design (35° minimum angle, 7° resolution) should permit an excellent comparison with QED theory.

It should be noted that absolute cross-section measurements are not required. The effect of a small-distance breakdown in QED may be represented by including a form factor in the Møller cross section, which can then be written as:

$$\frac{d\sigma}{d\Omega} = \frac{r_0^2}{8}\left(\frac{m_c^2}{E}\right)^2 \left[\frac{1+\cos^4(\theta/2)}{\sin^4(\theta/2)} F^4(q^2) + \frac{1+\sin^4(\theta/2)}{\cos^4(\theta/2)} F^4(4E^2 - q^2) + \frac{2}{\sin^2(\theta/2)\cos^2(\theta/2)} F^2(q^2)\, F^2(4E^2 - q^2)\right],$$

where the first term in the square bracket represents the direct scattering, the second the exchange, and the third the interference between the two, and q is defined as $q = 2E \sin(\theta/2)$. With 500-Mev electrons in the storage rings, the counters (35° to 90°) cover a range of q from 300 to 700 Mev/c. By running the experiment at other electron energies,

other ranges of q can be covered. The experiments at different electron energies can be relatively normalized from the data on the assumption that QED does not break down ($F = 1$). Any deviation from the predicted curve would indicate a breakdown in the theory. Since the cross section increases rapidly with decreasing electron energy, very good statistics can be obtained on the low-energy runs with only a small increase in running time.

During the past two years a number of foreseeable experimental problems have been considered. Those of importance are outlined in section III, and brief summaries of the corresponding calculations are contained in the appendices.

III. OUTLINE OF EXPERIMENTAL PROBLEMS

In this section brief descriptions will be given of the major questions on the feasibility of the experiment. The results of the corresponding calculations are given in the appendices. In general, the results of these calculations have set the design of the experiment and have determined the cost.

The accelerator beam is about $\frac{1}{4}$ in. in diameter, diverging at an angle of less than 10^{-4} radian. The energy spread is 2%, and the average current up to $\frac{1}{2}$ μa. At present its pulse length cannot be made less than 100 mμsec. To be conservative, we assume an 0.1-μa average current and a 100-mμsec pulse, although modifications of the accelerator gun to permit obtaining the full charge per pulse in 2×10^{-8} sec are believed possible.

The delay-line inflector (Appendix A) has a 1.1-cm vertical aperture. Under optimum conditions it should accept the full beam for about 1.4 turns, or 5.5×10^{-8} sec. We assume the effective acceptance time to be 8×10^{-9} sec as an additional safety factor. The storage-ring energy acceptance region will be at least 2.5-Mev wide (Appendix C), or $\frac{1}{2}$% of the accelerator beam energy. Roughly half the circumference is within the stable phase region. Injecting on every accelerator pulse, the effective current adding electrons to a ring is $10^{-7}/(12 \times 4 \times 2 \times 3) = 0.3 \times 10^{-9}$ amp, in which an added safety factor of 3 is included. The time t required to reach a 1-amp ring current is then $t = (3 \times 10^{9})/f$ where f is the circulation frequency; $t = (3 \times 10^{9})/(0.25 \times 10^{8}) \approx 120$ sec. Since the expected beam lifetime is at least many minutes (design value, 30 hours), the requirements on the accelerator and inflector are modest.

Once in the ring, the electrons must be guided by a field with good focusing and symmetry properties, well away from resonances. To accomplish this, each magnetic quadrant will contain end sections with $n = 0$ (no gradient) and a central region of positive gradient. The number of radial and vertical betatron oscillations per turn, Q_R and Q_V, will be

0.77 and 0.88, respectively, with $n_1 \sim 1.10$ (Appendix B). This cell structure will prevent problems as to the sign of the field gradient in the common magnet sections adjacent to the experimental straight section.

The field required for 500 Mev, 12 kilogauss, will be obtained from a magnet of conventional "H" design, made of large steel plates. This plan permits considerable flexibility in obtaining extra γ-ray beam holes or observation ports. The coils are of a simple flat shape, requiring no bends out of a plane. The total iron and copper weight for two rings will be about 46 tons, and the total dc power 450 kw. Magnet ripple and regulation will be unimportant, since the radius of the circulating beam is set by the r-f frequency; the effects of magnetic field changes will wash out in a radiation damping time, 10 msec (Appendix D).

Once an electron beam is captured, there are several effects leading to its loss. In the order of their estimated importance, they are:

(1) Quantum fluctuations leading to synchrotron oscillations (Appendix E). The synchrotron oscillations will, at 500 Mev, have an equilibrium width of 0.3 cm and will occupy $\sim 21°$ in phase. The loss rate due to the leakage of electrons over the phase-stable potential barrier has been calculated by Christy, and checked roughly by measurements on the Cal.Tech. electron synchrotron. With an r-f system operating on the fundamental circulation frequency, the calculated lifetime against losses at 20-kv peak r-f voltage is many years. At 12 kv the loss time drops to ~ 100 sec. The design value is 20 kv.

(2) Losses due to bremsstrahlung. The radiative scattering of circulating electrons from nuclei of the residual gas leads to additional energy fluctuations from the equilibrium value. It can be shown (Appendix F) that the only important radiative process is that in which the electron loses, in one event, enough energy to be lost from the phase-stable region. A fractional energy loss of one part in 400 could probably be tolerated, but the calculation assumes for safety that 1/1500 leads to loss of the radiating electron. The mean distance of travel before a single radiative event of $E_{max}/1500$ is about 1/7 radiation length. At 10^{-6} mm Hg this lifetime is 2 min.; at the design value of 10^{-9} mm Hg, it is 30 hours.

(3) Losses due to multiple gas scattering, nuclear interactions, and quantum fluctuations leading to betatron oscillations. All these can be shown to be small. Due to the strong radiative damping, the beam size set by gas scattering is only 40 μ even at 10^{-6} mm Hg (Appendix F). According to Christy, the vertical beam size due to quantum fluctuations is only a few microns (the fluctuations do not couple directly into the vertical oscillations). The radial betatron oscillations (Appendix F) are 0.3 cm due to the fluctuations; however, the loss rate depends on the value of the betatron oscillation density function at the nearest wall. This function is reduced from the central density by a factor of $\sim 10^{-300}$, and the corresponding loss rate should be quite undetectable.

(4) Losses due to interaction-region forces. The space charge limiting current density for electrons of 500 Mev in a 12-kilogauss guide field is far larger than the 1 amp/0.05 cm^2 maximum this experiment is designed for. However, the opposing electron beam in a colliding-beam system cancels part of the magnetic attractive force in the crossover region. Federbush has shown (Appendix G) that the effect would lead to an increase in vertical beam size with head-on beam collisions, and to possible beam instabilities that might result in rapid loss of the beam. If the beams collide at an angle, the only instabilities we have been able to find vanish. The remaining effect is a slight distortion of the beam shape--in fact, a reduction in the effective crossing angle. This would lead to an increase in the useful counting rate. At the crossover angle planned, there should be a considerable safety factor against any instabilities. Although this effect has received our greatest attention, it remains the only unfamiliar element in the theory of operation of the experiment. Fortunately, we could tolerate a reduction of a factor of 10 in circulating beam current if it were forced on us by unforeseen stability requirements.

(5) Trapped-ion effects. The circulating electron beams will ionize residual gas atoms, and the positive ions formed would be trapped by the electric field of the beam. It can be shown (Appendix I) that an average field of 400 v/cm exists near a 1-amp ring current. The alteration of focusing forces by these trapped ions would lead to instabilities. We plan to prevent all such effects by providing insulated metal floor plates

in the vacuum chamber, biased to 3 kv, which would sweep out ions in a fraction of a microsecond. As an incidental effect, this system should have a strong ion pumping action (Appendix I), and should lead to even better vacua than can be provided by the liquid-nitrogen-trapped oil pumps.

(6) Vacuum system. The detailed design of the vacuum system has been carried out with the advice of the Project Matterhorn ultrahigh-vacuum system group. It is an odd fact that the pumps for ultrahigh-vacuum work are much smaller than those for conventional systems. It will be necessary to assemble the 4000-lb vacuum chamber on a supporting frame, surround it with a low-temperature oven, and bake it out at 400°C. It will then be lowered into place, and the top coils and magnet halves assembled afterward. According to Grove's data,[13] we should get vacua of 10^{-9} mm Hg or better.

(7) Beam monitoring. The beam current and phase width in each ring can most conveniently be measured by a conventional pickup electrode. Sections of the insulated floor of the vacuum chamber will be used for this purpose. An additional rough measurement of total beam current can be obtained from the temperature rise of the vacuum-chamber cooling water; about 4 kw per ring of radiated power will be carried off by this cooling system at 1 amp of ring current. The equilibrium orbit in each ring can most accurately be plotted by search coils or current-carrying wires, since the magnets will be operated at constant field. Point-by-point measurements of electron beam vertical position under operating conditions can also be made. Remote-viewing ports at several locations have been designed to allow visual location of the beam to 1-mm accuracy.

IV. TIME SCHEDULE AND COOPERATIVE ARRANGEMENTS

The performance of the experiment is a cooperative effort by staff members of Stanford and Princeton Universities. Responsibility for the pulsed inflectors, the r-f equipment, and the vacuum system, is being taken by Princeton. The Stanford group has assumed responsibility for all fixed-field magnets, the experimental building, and the particle detection equipment. An estimated time schedule for the experiment is shown in Table IV-1.

The major equipment items are in the process of design or construction as follows:

Storage-ring experimental area — Construction of a shielded experimental area, a concrete "vault," behind the present Mark III target area began on 6 April 1959. The estimated completion date is 31 July 1959. The area will be 39-ft wide and 38-ft deep, with a floor at the same level as that of the Mark III target area. An entry adjoining but separate from the present target area entry will be constructed. The entryway will be covered to provide space for delivery and assembly of large equipment.

Storage-ring magnets — The magnets were designed at Stanford, and bids for their construction have been received. The first magnet should be delivered in November 1959, and the last in January 1960.

Injection magnets — The dc magnets for bending the beam into the rings have been designed.[14] Bids for their construction will be requested by the end of July 1959.

Vertical beam-steering magnets — An instrument for measuring the direction of the total momentum transferred to the beam by one of the vertical steering magnets has been constructed. Tests of a model magnet with empirically-shaped pole pieces have shown that the momentum transferred will be uniform in direction within 1° for any orbit passing within an area

4.3-in. wide and 1.6-in. high. Refinement of the pole shaping will probably produce a uniformity of 0.5° in the deflection produced by the actual beam-steering magnets.

Particle detectors — No work has been done to date on the construction of the detectors. A 256-channel pulse-height analyzer has been purchased by the High-Energy Physics Laboratory and will be used for multi-channel data storage. It is planned to assemble and test counters during the time necessary for the study of beam dynamics.

Storage-ring vacuum chamber — The chamber has been designed at Princeton, and materials for its construction have been ordered. The required special steel is scheduled for delivery in June 1959. A bake-out oven of 50 kw at 208 v is being designed. The vacuum chamber and its associated equipment should be moved to Stanford late in 1959.

Pulsed inflectors — Most of the components for the pulsed inflectors have been acquired and tested at Princeton. Assembly of the system will begin at Stanford during the Summer 1959.

R-f system — The design has been completed at Princeton, and almost all the required parts have been ordered. The r-f cavities and some of the electronic assemblies are being built in Princeton shops. The final assembly of the r-f system will be done at Stanford during the time G. K. O'Neill is in residence here (June 1959 - January 1960).

TABLE IV-1. Estimated time schedule

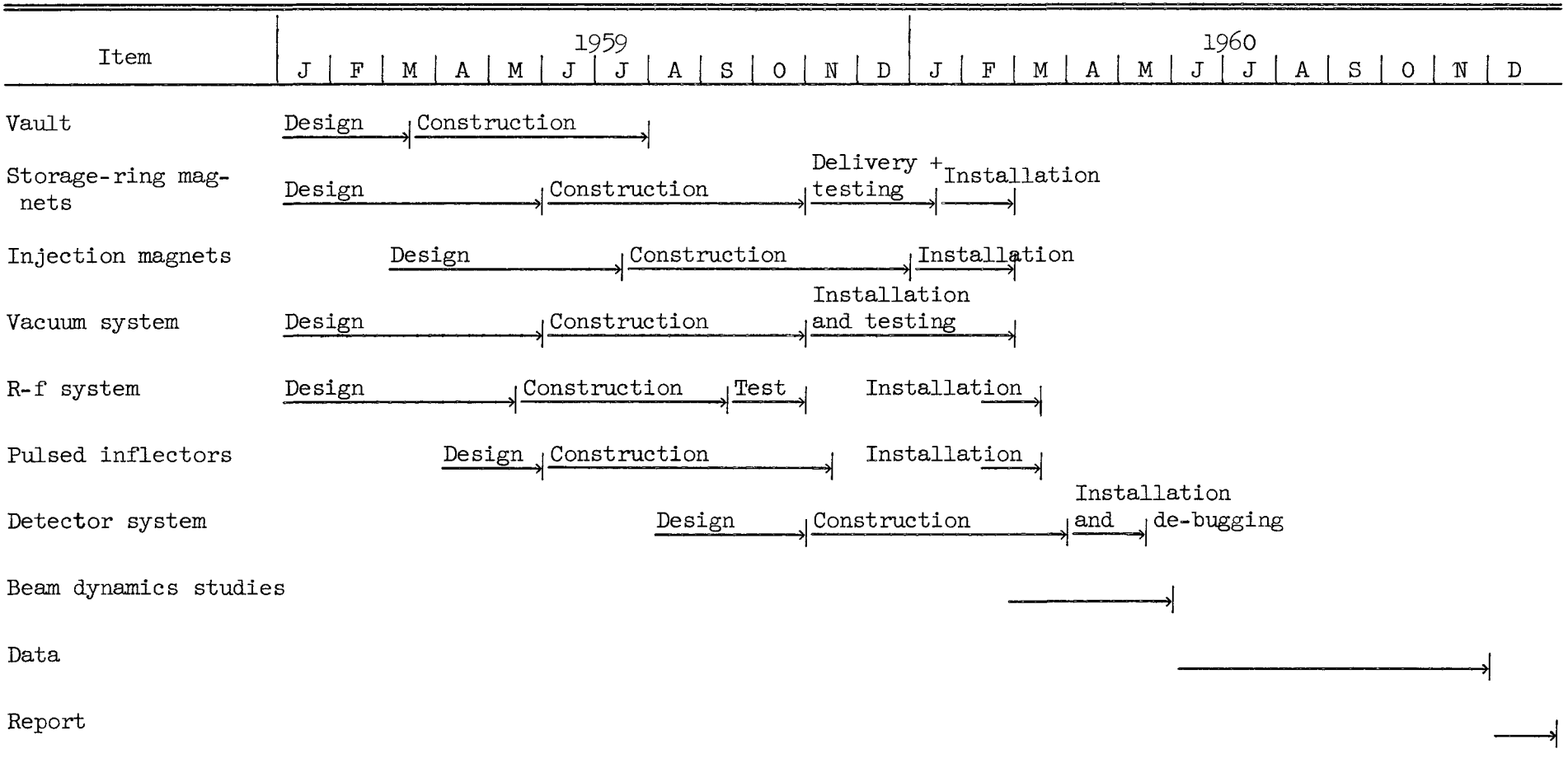

V. TABLE OF PARAMETERS

Electron energy	500	Mev
Storage-ring magnets		
Total weight	46	tons
Total power	450	kw
Gap field	12 000	gauss
Gap height	2.5	in.
Gap width	10	in.
Orbit radius	56	in.
Straight-section length	28	in.
Orbit length	464	in.
N-value	1.10 and 0.00	
Injection magnets		
Total weight	4.5	tons
Power for single 30° magnet	19	kw
Power for double system (120°)	63	kw
Gap field	12 000	gauss
Gap height	1.25	in.
Radiofrequency system		
Frequency	25.4	Mc
Frequency stability	1 part in 10^4	
Cavities/ring	1	
Peak cavity voltage	20	kv
Cavity Q	5000-1300	(controllable)
Cavity losses (2 cavities, approximate)	4-14	kw
Power to beam (2 rings)	8	kw
Maximum power to beam in 1 ring	9	kw
Amplifiers (type 4CW10000)	2	
Beam dimensions		
Radial width (calculated)	0.32	cm
Vertical height (max)	0.1	cm
Length	70	cm
Beam properties		
Stable phase angle	12°	
Phase spread	21°	
Radiation loss per turn	4.1	kev
Typical quantum energy	214	ev
Oscillation amplitude damping times		
betatron vertical	10×10^{-3}	sec
betatron radial	10×10^{-3}	sec
synchrotron	5.0×10^{-3}	sec

[Beam properties (continued)]

Oscillations/turn		
vertical	0.88	
radial	0.77	
Circulating beams (design value)	1	amp/ring
Lifetimes		
quantum fluctuations (calculated at 20 kv)	10^{10}	hours
bremsstrahlung (calculated for 10^{-9}mm air pressure)	30	hours
single gas scattering (10^{-9} mm)	200	hours
Beam crossing angle (vertical)	0.03	radian

Inflection

Pulsed magnet	(ferrite delay line)	
Pulse voltage	25	kv
Acceptance time	55×10^{-9}	sec
Number of turns injected	1.4	
Beam deflection angle	0.06	radian
Aperture height	1.1	cm
Aperture total width	3	cm
Energy acceptance	0.6	%
Inflector power	1250	watts

Vacuum system

Materials	stainless steel, ceramics	
Bakeout temperature	400	°C
Design pressure	10^{-9}	mm Hg
Maximum tolerable pressure	10^{-7}	mm Hg
Radiated power absorbed	8.2	kw
(Radiated power)/(orbit length)	9	w/in.

Detection

Minimum angle	35°	
Total number of counters	100	(maximum)
$d\sigma/d\Omega$ (35°)	2.4×10^{-30}	cm^2
$\Delta\Omega$ at 35°	0.18	sterad
Count rate at 35° (1-amp beams 0.5-cm wide)	1.3	counts/sec
$d\sigma/d\Omega$ (85°)	0.18×10^{-30}	cm^2
$\Delta\Omega$ at 85°	0.62	sterad
Count rate at 85°	0.32	counts/sec

APPENDIX A

DELAY LINE INFLECTOR*

Over most of the injection path, the electrons will be guided by a dc field, obtained by shaping a magnetic channel through one quadrant. Once out of the channel (Fig. A-1) they will perform part of one betatron oscillation before entering the next straight section. We then require the pulsed magnetic field to reduce the amplitude of the betatron oscillation, so that on subsequent turns the electrons will not strike the magnetic channel. In order that an electron be injected successfully, we must also require the pulsed field to be off before the electron meets it a second time. If the betatron oscillation amplitude is written $A = A_0 \cos\theta$, with $\theta = 0$ just after the first passage through the pulsed field, the amplitude one turn later is $A_1 = A_0 \cos 2\pi Q_R$, where Q_R is the ratio of the radial betatron to the rotation frequency. If we choose $Q_R = 0.77$ by setting $n_1 = 1.10$ (cf. Appendix B), then

$$A_1 = A_0 \cos 2\pi\ (0.77) = A_0 \cos(83°) = 0.12\ A_0\ ,$$

$$A_2 < 0\ ,$$

$$A_3 < 0\ .$$

The electrons will therefore clear the pulsed field after the first turn (Fig. A-2). However,

$$A_4 = A_0 \cos 2\pi\ (3.08) = A_0 \cos(28°) = 0.88\ A_0\ .$$

The fourth turn will therefore return to hit the inflector field, so the field must be reduced to zero in less than four turns. It is designed to turn off in two turns (80 mμsec); the acceptance time for incoming electrons will then be ~ 55 mμsec when the finite pulse rise time is included.

---

*See reference 12.

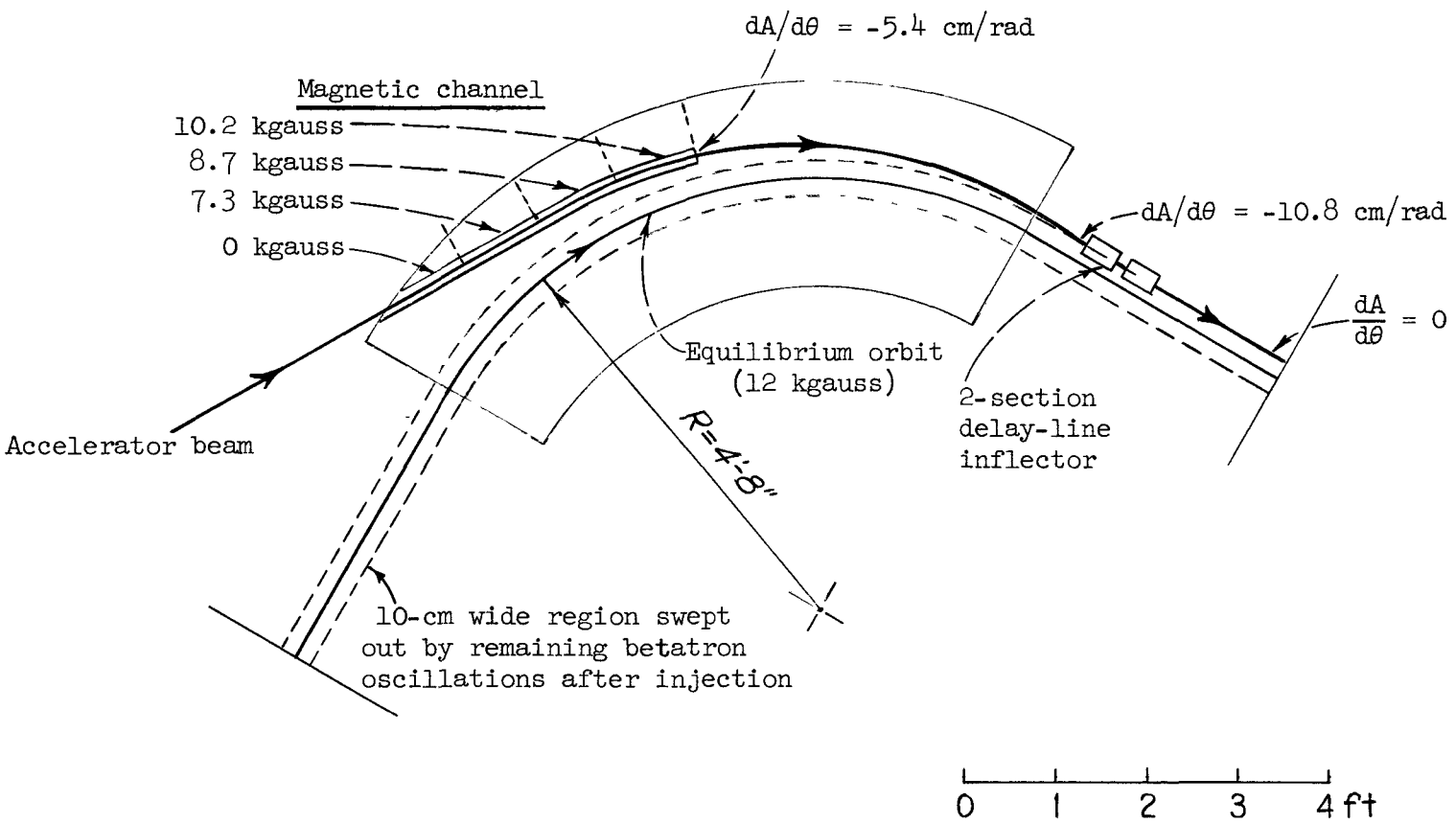

FIG. A-1.-- Magnetic channel and pulsed inflector for injecting electrons into the storage rings.

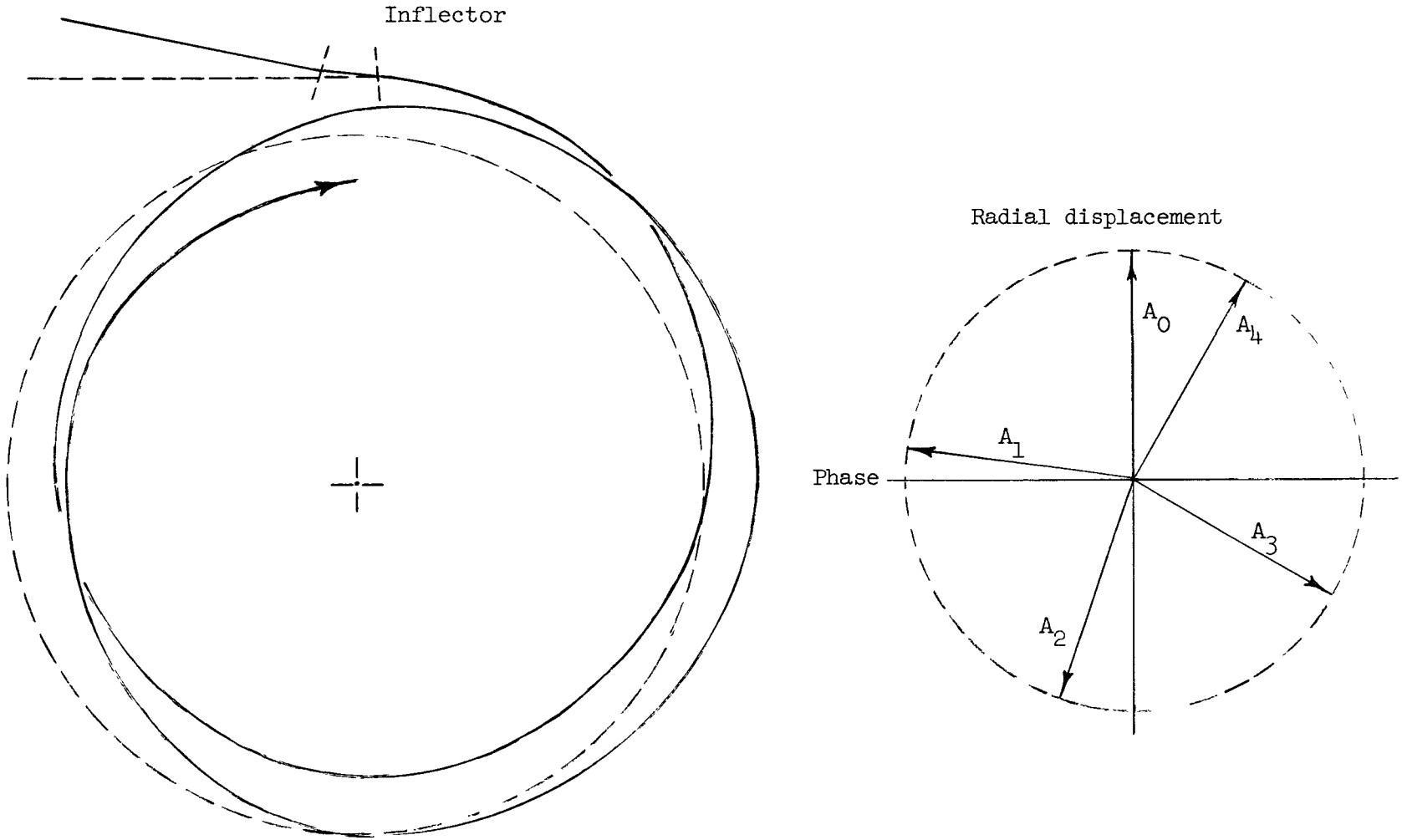

FIG. A-2.-- Curves illustrating the motion of electrons in the storage rings immediately after injection. The vectors $A_0, \ldots A_4$ represent the amplitude and phase of the radial betatron oscillations at the inflector position on successive turns.

During the 16-msec interval between injection pulses, the radiation damping of the radial betatron oscillations will reduce A_0 to 1 cm; the inflector can therefore be pulsed on without affecting the previously stored beam.

The pulsed magnetic field (2400 gauss over a 42-cm length) could be supplied by a single-turn coil. By applying an input voltage of 100-kv amplitude and complicated shape, the magnetic field could be made to hold constant for a time, then drop to zero in 80 mμsec. The control problem would, however, be quite difficult. Furthermore, an air-core coil would produce a large stray field at the radius of the circulating beam. We plan instead to use a C-shaped ferrite magnet (Fig. A-3) which can produce a uniform magnetic field within its gap. The stray field from such a geometry should be small. At short intervals along the one-turn exciting winding, condensers will connect opposite sides of the loop. These condensers together with the inductance of the gap will form a delay line with a characteristic impedance of 11 ohms (Fig. A-3). By terminating this line with a resistor, and driving it from a charged coaxial cable through a spark gap, the fast control problem will be avoided and the desired wave-form can be produced. With a deflection angle $\theta = eB\ell/p$ for electrons of momentum p (in MKS units), ℓ the length of the magnet of gap field B; the pulse current required is $I = Hh = Bh/\mu_0$, where h is the gap height and μ is assumed much larger than μ_0. The inductance per unit length is $L' = \mu_0(w + h)/h$, where w is the effective gap width. The line impedance is $Z_0 = L'/\tau' = \tau'/c'$, and the pulse voltage is $V = IZ_0 = (p\theta/e\tau')[(w+h)/\ell]$ $= (p\theta/e\tau)(w + h)$, where τ is the delay time through the line.

We are permitted an additional choice of impedance by splitting our inflector into several short delay lines, driven in parallel. We choose V = 25 kv, to hold the peak dc charging voltage to 50 kv. The spark gap will operate well at this voltage, and 50 kv is easily obtained from commercially available power supplies.

At 500 Mev, $p/e = 1.67$. With $\tau = 80$ mμsec and $(w + h) = 4$ cm, $\theta = 0.03$ rad/section.

The electrons will emerge from the magnetic channel halfway through one quadrant, 10 cm from their equilibrium orbit. Writing the subsequent

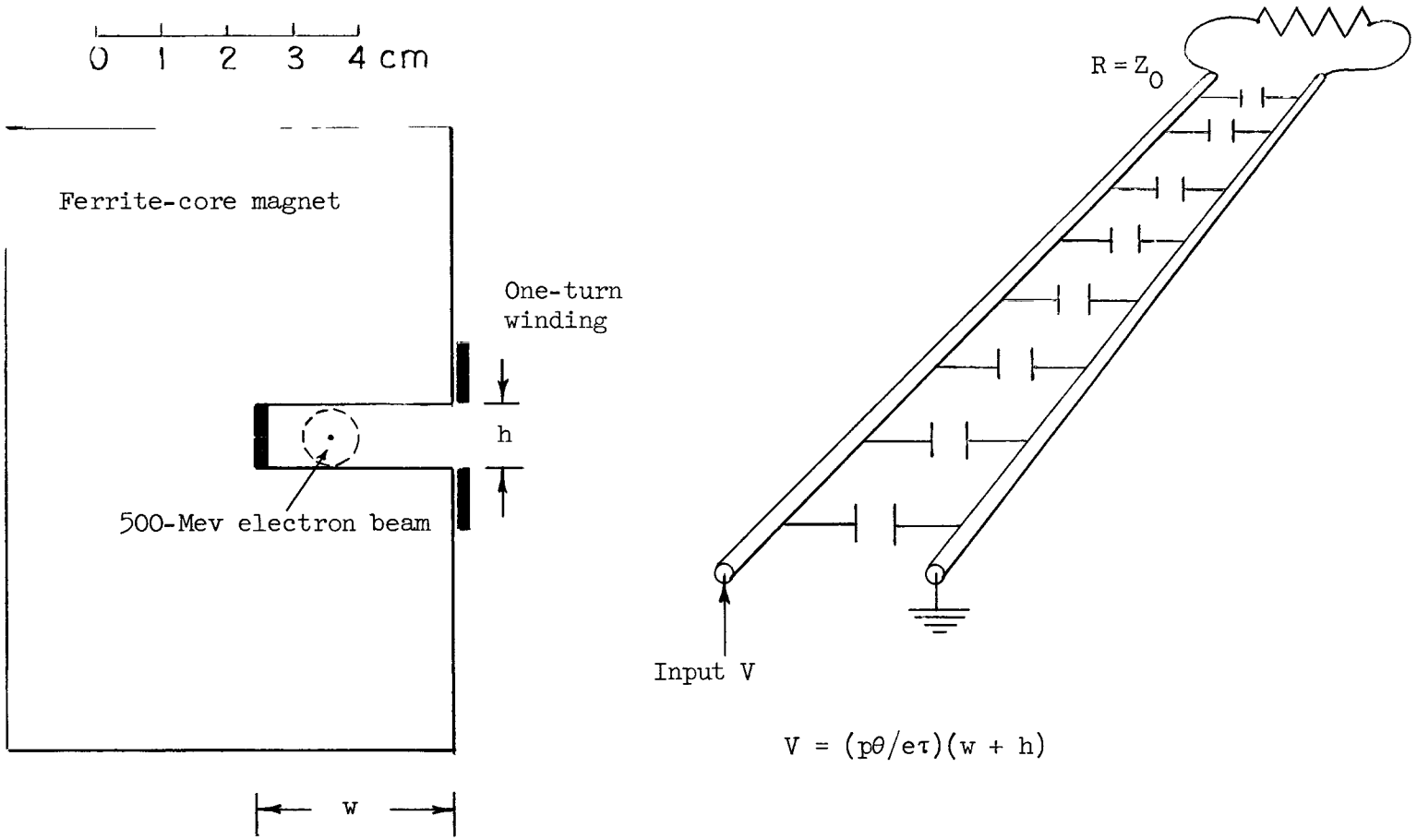

FIG. A-3.-- Details of the pulsed inflector

betatron oscillation as $A = A_0 \cos(\theta + \delta)$, with $\theta = 0$ at the channel end, we must have $A = 5$ cm when $\theta = 36°$, the location of the inflector. From these conditions, $A_0 = 11.4$ cm and $\delta = 28°$; $dA/d\theta = -10.8$ cm/rad at the inflector, and $\mathcal{R}_{betatron} = 217$ cm. The deflection angle must therefore be 0.06 radian, and the pulsed magnet must be cut into two sections. Using $\ell = 21$ cm/section, $\tau' = 4$ mμsec/cm, and $Z_0 = 11$ ohm/section. The pulse current will then be 2300 amp/section, and the gap field 2.4 kgauss. This field is within the range for ferrites, which saturate at 3.6 to 5.1 kgauss. Driving both sections in parallel, the peak current will be 4600 amp; with 145-mμsec pulses at a 60-cycle rate, the inflector power will be 1000 watts, requiring a 2000-watt power supply.

APPENDIX B

MAGNET CELL STRUCTURE

With the magnetic gap field downward, electrons will circulate clockwise in each storage ring. At the ends of the interaction straight section, there will be magnets common to both rings. In the common regions, any field gradients would have opposite signs for the two rings. We cannot therefore use the same gradient in all magnetic field regions. To preserve simplicity and a high degree of symmetry, we will treat all quadrants in both rings alike: each will consist of end sections with $n = 0$, and a central section with $n = n_1$. The $n = 0$ regions must be ~38-cm long if a 15-cm annular width in one ring is to clear the positive-gradient region of the other ring. Then n_1 must be chosen to avoid betatron-oscillation resonances, given by $mQ_V + nQ_R = p$, where Q_V and Q_R are the numbers of vertical and radial oscillations per turn, and m, n, and p are small integers. Approximate formulas for Q_V and Q_R are

$$Q_V = [n(1 + \alpha_1)]^{\frac{1}{2}},$$

$$Q_R = [(1 - n)(1 + \alpha_2)]^{\frac{1}{2}};$$

here the α's are the ratios of nonfocusing to focusing lengths, and $(1 - n)$ must be weighted by the lengths of $n = 0$ and $n = n_1$ sections. No vertical focusing occurs for $n = 0$. As expected, Q_R is given quite accurately by the expression above, but the smooth approximation involved gives only a qualitative answer for Q_V. Correct values can be obtained by expressing a transformation matrix for each magnetic cell, and multiplying matrices over a symmetry unit. Following this method, Korenman has obtained the graph of Fig. B-1 for Q_V and Q_R as functions of n_1, assuming a symmetry of four per revolution. Existing synchrotrons operate successfully through resonances $Q_V = 2/3$ and $3/4$, and $Q_V = Q_R$, so the

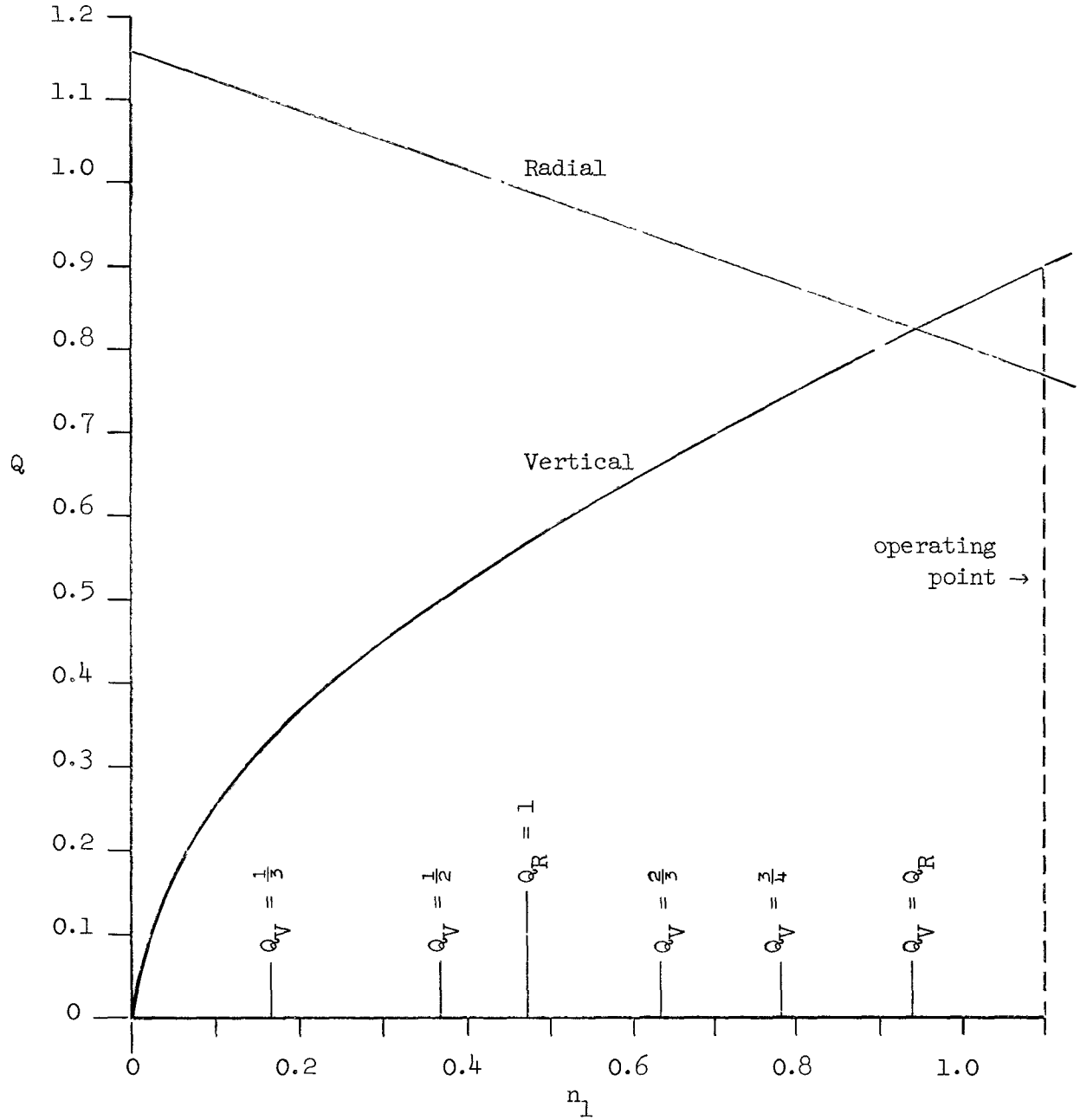

FIG. B-1.-- Curves showing the number of radial and vertical oscillations per turn, Q_R and Q_V, as a function of the n-value in the non-uniform field regions of the storage rings.

available operating regions are wide. The value $n_1 = 1.1$ may be a good choice. Since n_1 is set by small shims, it need not be chosen before the magnets are built.

Vertical steering. By inserting magnetic fields in the median plane at opposite ends of the interaction straight section, the electron beams can be made to cross at a small angle at the midpoint. Operating with $Q_V = 0.88$, the perturbed equilibrium orbit can be found. Outside the interaction straight section it will consist of almost 0.88 of a vertical betatron oscillation stationary in space (Fig. B-2). The uniqueness of Fig. B-2 is forced by symmetry and the fact that the magnetic steering fields are equal and opposite. If we make a smooth approximation for the guide field, the amplitude outside the interaction region can be written $A = A_0 \sin\theta$. At the steering magnet position, $A = \varphi\ell/4$, where φ is the crossover angle. At that point, with $Q_V = 0.88$ and $\ell \ll 2\pi r$, $\theta = \pi - 0.88\pi = 0.12\,\pi$, so $A = 0.4\,A_0$. The maximum displacement of the equilibrium orbit is therefore $2.5(\varphi\ell/4)$. With $\varphi \sim 0.03$ and $\ell = 37$ cm, this displacement is 0.7 cm. The steering magnets must produce a field of 3 kgauss effective over a 10-cm path, with good uniformity.

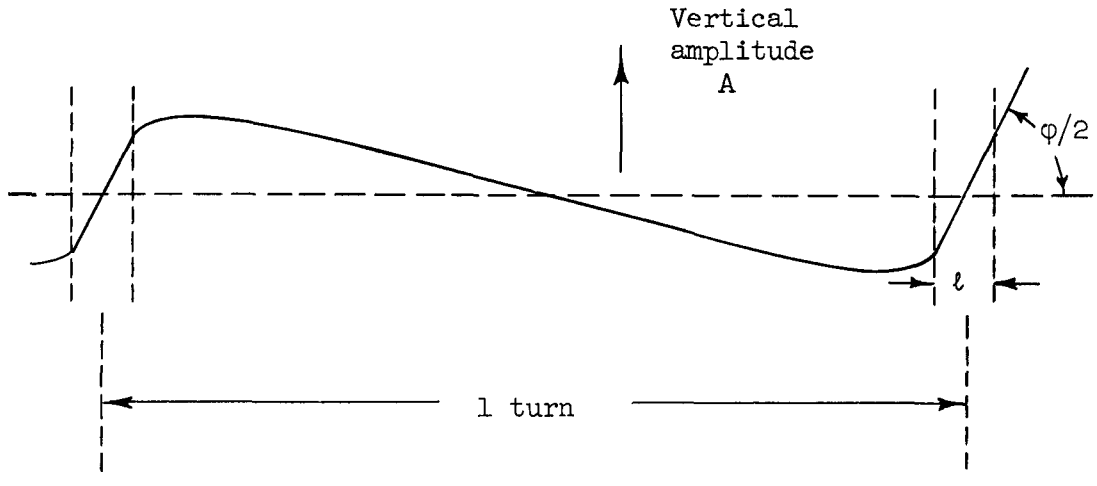

FIG. B-2.-- Vertical equilibrium orbit

APPENDIX C

CAPTURE EFFICIENCY

Section III contains a discussion of the electron capture rate, depending on Appendix A for the inflector properties and on this section for the storage-ring energy acceptance.

We can obtain the maximum energy acceptance in two ways. The first is to observe the equilibrium radial spread (Appendix D), and to note that in calculating the quantum fluctuation loss rate according to Christy[11] the ratio $E_m/(q/\beta)$ is ~15 for our parameters, and is the ratio of the separatrix Δr to the equilibrium Δr of the beam. The storage rings can therefore contain a synchrotron oscillation amplitude $\Delta r \sim 15(0.15 \text{ cm}) \sim 2 \text{ cm}$, or $\Delta E/E_0 \sim \pm 1\%$.

We can also note that the synchrotron oscillation frequency is

$$\Omega = \omega_0 \left[\frac{eV}{2\pi E_0 (1 - \bar{n})} \right]^{\frac{1}{2}} ,$$

where ω_0 is the rotation frequency, V the r-f voltage, and $E_0 = 500$ Mev. At 20 kv,

$$\Omega/2\pi \approx (0.4 \times 10^{-2})(\omega_0/2\pi) \sim 110 \text{ kc} .$$

The phase velocity in synchrotron oscillation is related to the displacement from the equilibrium orbit by

$$\dot{\varphi} = -\omega_0(\Delta r/r_0) .$$

Linearizing the synchrotron oscillations,

$$(\varphi - \varphi_s) = A \cos\Omega t .$$

The stable phase limit is

$$\varphi_{max} = \pi - \varphi_s ,$$

so that $A \approx \pi$ for $\varphi_s \sim 0$. Then

$$\dot{\varphi}_{max} \approx \pi\Omega \approx \omega_0(\Delta r_{max}/r_0) .$$

For our parameters,

$$(\Delta r_{max}/r_0) \approx (0.6 \times 10^{-2})\pi \approx 2 \times 10^{-2} ,$$

the same result obtained above. The storage rings can therefore accept electrons over nearly 2π in azimuthal angle, with an acceptable radial full width going from zero at the separatrix ends to 4 cm near $\varphi = \varphi_s$. With $(\Delta p/p) \approx 0.5(\Delta r/r)$ for our n-value, the rings can accept an energy spread of ~2% maximum. If, due to aperture restrictions set by the inflector, we require a maximum synchrotron oscillation amplitude of 1 cm, roughly half the circumference is within the corresponding region in phase.

APPENDIX D

RADIATION DAMPING TIMES AND BEAM SIZE

The damping time for synchrotron (phase) oscillations has been calculated by several authors to be[15-18]

$$\tau_S = 2 \frac{(1 - n)}{(3 - 4n)\rho} ,$$

where

$$\rho \equiv P_\gamma / E ,$$

and

$$P_\gamma = \frac{2}{3} \frac{e^4}{m^2 c^3} \frac{v^2}{c^2} B^2 \left(\frac{E}{mc^2} \right)^2$$

is the power radiated per electron in a guide field of constant index n; E is the whole energy of the electron. This damping arises from the increase in average energy loss per turn with increasing radius, given by P_γ. The damping strength can be calculated by considering a phase vector rotating in (r_{equil}, φ) space, where φ is the r-f phase angle. The equilibrium r-f phase angle φ_0 changes with instantaneous energy loss. A correct but somewhat more involved derivation is used in the references quoted, and has been summarized by Christy.[11]

The vertical oscillation damping arises because all vector components of the electron momentum decay in a time $1/\rho$, while the r-f replaces the energy loss of only the axial component. Since there is no dependence of the radiated power on vertical oscillation phase or amplitude, the vertical oscillation energy damping time is $1/\rho$, giving an amplitude damping time $\tau_V = 2/\rho$.

Two effects must be considered in the damping of radial betatron oscillations. The first, a decay of the oscillation amplitude due to radiated power, is identical to that of the vertical oscillations. The second is due to the increase of radiated power with decreasing radius,

given by the expression for P_γ. The electrons radiate preferentially when their instantaneous betatron phases bring them inside the equilibrium orbit. As summarized by Christy, the damping time is $\tau_R = 2(1 - n)/\rho n$.

The existing calculations apply to guide fields of constant n (straight sections increase the damping times only by reducing the fraction of time the electrons radiate). In our case n fluctuates rapidly between 0 and ~1.0. This should not affect τ_V, in which n does not appear. However, we must find whether our guide field is equivalent in its effect on radiation to a constant-n field with some effective average n-value. We show first that the orbits in our varying-n guide field are almost indistinguishable from circles (scale drawing and discussion on Fig. D-1). For a deviation Δp of the momentum from the central value p_0, $\overline{\Delta r}/r \approx 1.92(\Delta p/p_0)$. Neglecting the small (~4%) deviation of Δr from its average value at various azimuths in the magnet, the same value of "momentum expansion" would be obtained in a constant-n guide field with $n = 0.48$.

Except for the simple decay-damping of radial oscillations (unaffected by n), the only dependence of damping on n-value arises from the dependence of radiated power on radius. We are permitted to consider the average power radiated per magnetic cell (1/8 turn) since there are ~10 cells per betatron oscillation.

Using $P_\gamma \propto E^2B^2$, and $E_\theta = P_\gamma/\omega$, where E_θ is the energy loss per radian, one can add the energy radiated in each segment of a unit cell to find

$$dE_\theta/dr = (2\pi P_\gamma/c)(3 - 4\overline{n}) ,$$

with $\overline{n} = n/2$, and n the gradient in the center half of each quadrant. For constant n, one finds the same expression. The familiar condition $n < 3/4$ for damping of synchrotron oscillations appears here as a restriction that dE_θ/dr be positive.

For radial betatron oscillations one must show that the variation of E_θ with r (E held constant) is the same for constant and varying n-values. For both cases one finds

$$dE_\theta/dr \propto (2E^2B^2/\omega r)(-n) ,$$

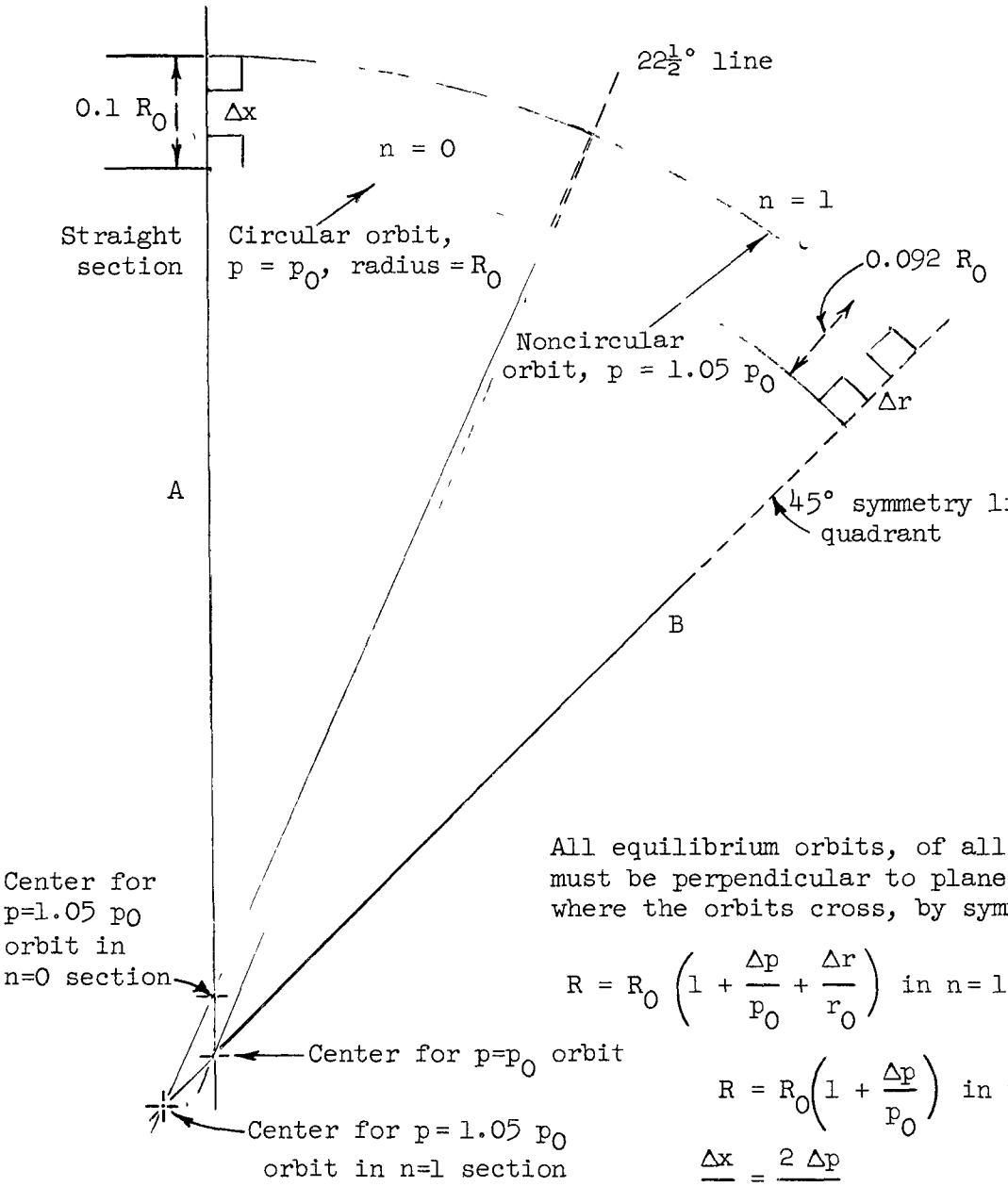

All equilibrium orbits, of all momenta, must be perpendicular to planes A and B where the orbits cross, by symmetry.

$$R = R_0\left(1 + \frac{\Delta p}{p_0} + \frac{\Delta r}{r_0}\right) \text{ in n = 1 section}$$

$$R = R_0\left(1 + \frac{\Delta p}{p_0}\right) \text{ in n=0 section}$$

$$\frac{\Delta x}{R_0} = \frac{2\,\Delta p}{p_0}$$

$$\frac{\Delta r}{R_0} = \left(2\cos\frac{\pi}{8}\right)\frac{\Delta p}{p_0} = 1.84\left(\frac{\Delta p}{p_0}\right)$$

FIG. D-1.-- Particle orbits in a guide field with two different values of n.

(This figure and the associated calculations were made for magnet sectors with n = 1 and n = 0, but the conclusion will be unaffected even though the final choice of n-value for the non-uniform sections will probably be closer to n = 1.1.)

where in our case $n \to \bar{n} = \frac{1}{2} n_{central}$. Therefore both for radial betatron and phase oscillations, we can expect damping corresponding to a conventional guide field of $n \sim 0.5$. It happens that Q_R obtained from the accurate matrix-multiplication (Appendix B) is also almost identical with that obtained from the ordinary $Q_R = [(1 + \alpha)(1 - n)]^{\frac{1}{2}}$, with $n = \bar{n} = 0.5$.

The radiated energy per turn in our guide field (including the reduction due to straight sections) is ~4 kev/turn at 500 Mev, so that with $f = 25.4$ Mc, $\rho = 210$/sec. Then $\tau_R \sim \tau_V \sim 10$ msec, and $\tau_S \sim 5$ msec.

Equilibrium beam size. Following Christy, the typical quantum energy is

$$E_\nu = \frac{3}{2}\hbar\omega\left(\frac{E}{mc^2}\right)^3 \sim 200 \text{ ev at } E = 500 \text{ Mev} .$$

There are then ~20 quanta/turn, and $P_\gamma\tau/E_\nu \sim 10^6$ quanta in one damping time. The amplitude of energy fluctuations is

$$\overline{\delta E^2} \cong E_\nu{}^2(P_\gamma\tau/E_\nu) = E_\nu P_\gamma \tau = (270 \text{ kev})^2 .$$

The associated amplitude of radial oscillations is $\delta r = (\delta E/E)[r/(1 - \bar{n})] \sim 0.10$ cm. For the radial betatron oscillations, using Christy's Eq. (6), p. 11, reference 11,

$$(\overline{\delta r^2})^{\frac{1}{2}} = (1.3 \times 10^{-5})(E/mc^2)[r_0(\text{cm})]^{\frac{1}{2}} .$$

At 500 Mev, with $r_0 = 140$ cm, $(\overline{\delta r^2})^{\frac{1}{2}} = 0.2$ cm. According to Christy, the quantum-induced vertical oscillations should be only (mc^2/E) as large as the radial.

Measurements of beam loss rate on the Cal.Tech. synchrotron have shown that the expression given above for synchrotron oscillations must be very nearly right; the radial betatron oscillations must also be not very much larger than those given by the theory. However, the vertical beam size in the Cal.Tech. synchrotron appears much larger (~5 mm) than the predicted vertical size.* Gas scattering cannot account for the additional

*Professor R. R. Wilson notes that the vertical beam size in the Cornell 1.2-Bev synchrotron is quite small (probably < 1 mm and possibly as small as the calculated value). Professor M. Sands notes that the apparent larger size of the Cal.Tech. synchrotron beam may be due to the optical viewing system's not being properly aligned with the circulating beam.

size, and it is difficult to find plasma effects which could produce this result at several hundred Mev. If some ion-trapping mechanism is responsible, it should be eliminated by our design of vacuum system (Appendix I).

APPENDIX E

BEAM LOSS RATE DUE TO QUANTUM FLUCTUATIONS

The effect of quantum fluctuations in the synchrotron radiation is equivalent to a noise source driving the phase and radial betatron oscillations. The combination of the radiation damping and quantum fluctuations leads to equilibrium beam sizes given in Appendix D. In addition, the fluctuations lead to particle loss, particularly through phase oscillations. A careful treatment of this subject by Christy[11] leads to an equation graphed in Fig. E-1. Measurements on the Cal.Tech. synchrotron indicate that the calculated r-f voltage for a given loss rate is correct within ~25%. Taking the most conservative interpretation of the measurement, the lifetime for losses due to phase oscillations should be many years at 20 kv. The minimum required r-f voltage (for a 2-min lifetime) is 12 kv.

Following Christy's notation, the radial betatron oscillation distribution should be proportional to $\exp[-(r - r_0)^2/2\delta\bar{r}^2]$.

With $r - r_0 = 5$ cm and $(\delta\bar{r}^2) = 0.13$ cm, as calculated, the distribution density at the nearest wall should be reduced from the central value by 10^{-300}. Even if the radial oscillation distribution is wider than the calculated value by a factor of three (there is no evidence for this from Cal.Tech. or Cornell measurements), the density distribution at the nearest wall should still be reduced by 10^{-30}, so losses due to this effect should be small.

The calculated vertical beam height is only 0.1 mm. At Cornell, where only rough measurements have been made, there is no evidence that the beam is much larger than this. However, at Cal.Tech. it has been measured as several millimeters high. Scaling down by the ratio of betatron wavelengths, we expect from Cal.Tech. results a height of ~1 mm. With more than 1 cm of clear vertical semi-aperture, the vertical oscillation

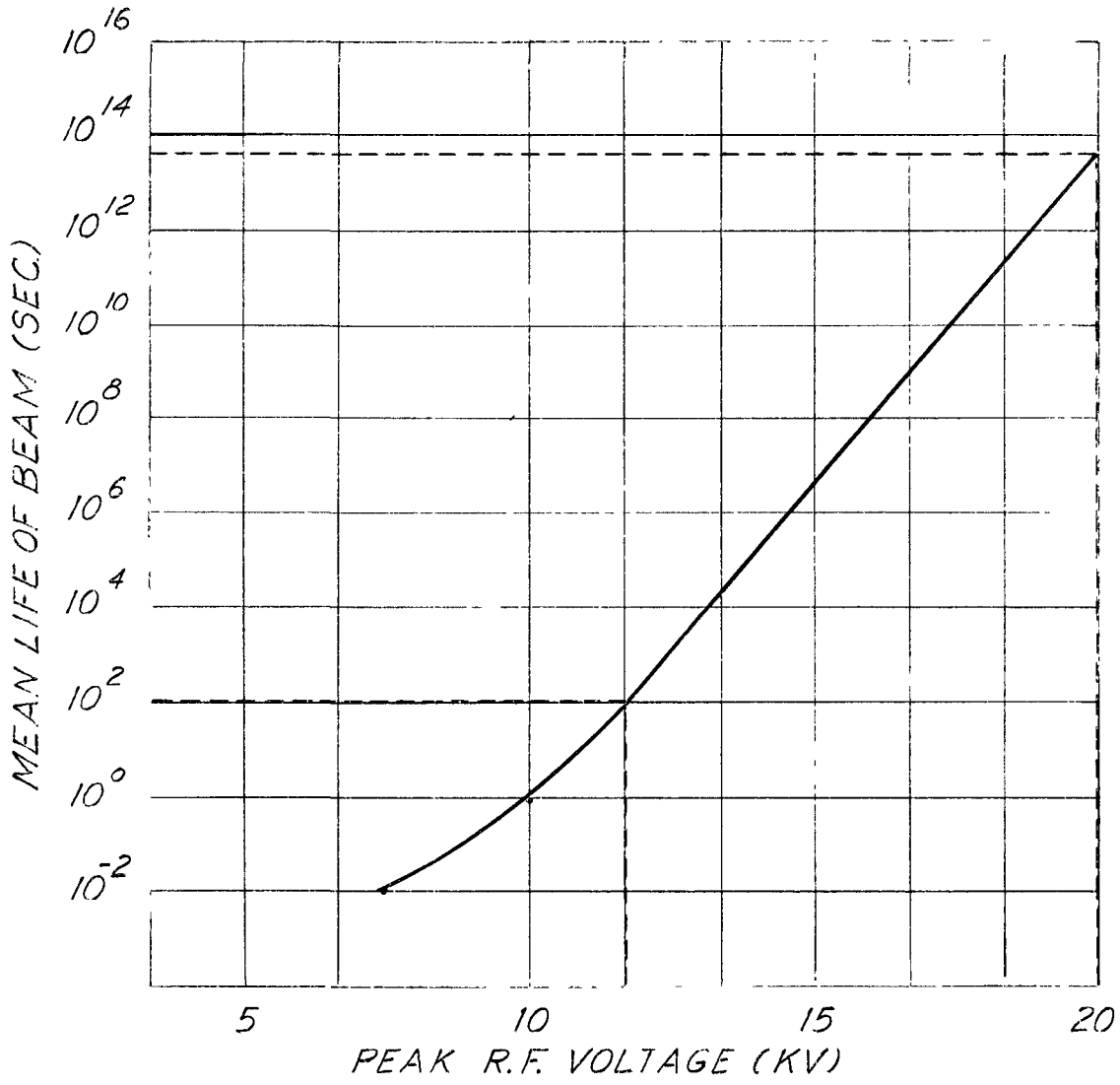

FIG. E-1.-- Beam lifetime due to quantum fluctuations as a function of r-f accelerating voltage (beam energy 500 Mev).

density distribution at the nearest surface should be reduced by $\sim 10^{-15}$ from the central value.*

*Professor Christy has very kindly checked that, according to his calculation, our beam lifetime should be some hours at 10^{-9} mm Hg. As he sensibly points out, however, one should be suspicious of very small Gaussians; we intend to obtain all information possible from existing synchrotrons, and allow generous safety factors in our design.

APPENDIX F

LOSSES DUE TO SCATTERING AND BREMSSTRAHLUNG

A. Gas Scattering

1. Multiple scattering

The statistical distribution in betatron oscillation amplitudes due to this effect has a width set by the gas pressure and by the damping rate. Following Ball,[19] the equation for vertical oscillations is

$$\ddot{z} + \rho_V \dot{z} + n\omega_0^2 z = 0 ,$$

where ω_0 is the rotation frequency and $\rho_V = P_S/E_S$, the fractional radiative loss per second. Solving,

$$z = A_0 \exp(-\rho_V t/2) \sin(n^{\frac{1}{2}}\omega_0 t + \delta) .$$

The distribution in amplitude as a function of time, $G(A,t)\,\partial A$, is obtained from the Fokker-Planck equation:

$$\frac{\partial G(A,t)}{\partial t} = -\frac{\partial}{\partial A}[f_1 G(A,t)] + \frac{1}{2}\frac{\partial^2}{\partial A^2}[f_2 G(A,t)] ,$$

where we define

$$f_1 = \lim_{\Delta t \to \tau} \frac{\langle(\Delta A)\rangle}{\Delta t} , \qquad f_2 = \lim_{\Delta t \to \tau} \frac{\langle(\Delta A)^2\rangle}{\Delta t} .$$

During τ, many scatters occur but A changes only by a small amount. By a substitution,[20] one can express f_1 and f_2 in terms of $D = \langle(\Delta\theta^2)\rangle/4\Delta t$, as $f_1 = (-\rho/2)A + (D/A)$; $f_2 = 2D$. Evaluating D,

$$D = (R^2/8n)(E_0/E_S)^2(cd/X_0) ,$$

where for our case $R = 142$ cm, $\bar{n} \sim 0.6$, $E_0 = 21.2$ Mev, $E_S = 500$ Mev; X_0 is the radiation length in g/cm^2, and d is the gas density. At 10^{-6} mm Hg, $D \sim 10^{-2}$ cm^2/sec. At 500 Mev, $\rho/2 = 10^2$/sec. The amplitude can then be shown to approach the stationary distribution $G(A) \sim \exp[(-\rho/4D)A^2]$, with A in cm. At 10^{-6} mm Hg the gas scattering beam size is therefore ~ 140 μ, the loss rate negligible. At 10^{-9} mm, the gas scattering size should be about 5 μ.

The horizontal oscillations due to gas scattering are the same except for a small constant related to n.

2. Single scattering

A single elastic scattering event will cause the scattered electron to be lost provided the angle of scattering is great enough. Because the vacuum chamber is narrow in the vertical direction, scattering in this plane will be the greatest source of loss. The scattering angle which leads to loss is given by

$$\theta = \frac{\frac{1}{2} \text{ vertical aperture}}{\lambda_{vert}} \approx 0.01 .$$

In a diatonic gas at NTP the number of elastic scatterings at an angle greater than θ per cm of gas path is given by

$$\frac{Z^2 \times 0.4 \times 10^{-5} \cot^2(\theta/2)}{E^2 \text{ (Mev)}} ;$$

with $\theta = 0.01$, $Z = 8$, and $E = 500$ Mev, this number is 4×10^{-5} cm^{-1}. At a pressure P the electron's mean free path due to single scattering is

$$\frac{760}{P} \times \frac{10^5}{4} \text{ cm} = \frac{1.9 \times 10^7}{P} \text{ cm} .$$

At a pressure of 10^{-8} mm Hg the beam lifetime due to this effect would be

$$\frac{1.9 \times 10^7}{10^{-8} \times 3 \times 10^{10}} = 6.3 \times 10^4 \text{ sec} .$$

B. Loss of Circulating Electrons Due to Bremsstrahlung

In the storage ring, the electrons are contained in a region of about 30° in phase angle, centered at 12°. The associated radial spread is about 0.3 cm, and the fractional momentum spread is 1/750. Electrons will escape from the separatrix if (a) a momentum change large enough to cause escape from the separatrix occurs in a single event, or (b) diffusion out of the separatrix occurs as a result of many successive small radiative events.

Process (a) is more important, and will be discussed first. In the approximation of a rectangular bremsstrahlung energy spectrum, the cross section per nucleus for radiating a photon of frequency ν^0 in $\Delta\nu^0$ is[21]

$$\Sigma(\nu^0)\,\Delta\nu^0 = \frac{1}{N\ell_r}\frac{\Delta\nu^0}{\nu^0},$$

where ℓ_r is the radiation length. The cross section for radiating a photon of frequency ν^0_{min} or greater is then

$$\Sigma(>\nu^0_{min}) = \frac{1}{N\ell_r}\ln\frac{\nu^0_{max}}{\nu^0_{min}}.$$

Here $h\nu^0_{max} = E_{electron}$, and $h\nu^0_{min}$ is the smallest energy loss which will result in escape of the electron from the separatrix. Since the circulating beam occupies a region surrounding the origin of synchrotron phase space, well inside the separatrix, we can safely take $h\nu^0_{min}/h\nu^0_{max} = \frac{1}{2}(\Delta p/p)$, where $\Delta p/p$ is the normal fractional momentum spread in the beam. Then,

$$\Sigma(>\nu^0_{min}) = \frac{1}{N\ell_r}\ln(1500) = \frac{7.3}{N\ell_r},$$

and the probability P per cm of escape is

$$P(>E_{rad}) = N\Sigma = 7.3/\ell_r.$$

In air at NTP, $\ell_r = 3.3 \times 10^4$ cm. The density of air at 10^{-8} mm compared to air at NTP is $10^{-8}/760 = 1.32 \times 10^{-11}$, so that for p = 10^{-8} mm,

$$\ell_r = \frac{3.3 \times 10^4 \text{ cm}}{1.32 \times 10^{-11}} = 2.5 \times 10^{15} \text{ cm} ,$$

and the lifetime against escape due to a single radiative event is

$$[cP(> E_{rad})]^{-1} = \frac{\ell_r}{7.3\ c} = \frac{2.5 \times 10^5}{7.3 \times 3 \times 10^{10}} = 1.1 \times 10^4 \text{ sec} = 3 \text{ hours} .$$

At a pressure of 10^{-6} mm, the lifetime would then be 2 minutes.

In the case of the quantum fluctuations in the classical synchrotron radiation, there is an important source of escape because the energy-loss time due to the radiated quanta is about equal to the damping time. In bremsstrahlung, when $x/\ell_r = 1/1500$, the electron has lost enough energy to move across the separatrix. However, this will result in escape only if the time is less than a damping time. At 10^{-6} mm, the time required for the electron to lose 1/1500 of its energy is

$$\frac{\ell_r}{1500\ c} = \frac{2.5 \times 10^{13}}{4.5 \times 10^{13}} \sim 0.5 \text{ sec} .$$

This is about 100 times as long as a damping time, so the bremsstrahlung diffusion process cannot be an important source of electron loss even at 10^{-6} mm.

APPENDIX G

INTERACTION REGION STABILITY

For particles traveling in the same direction on parallel paths, the magnetic attractive force nearly cancels the repelling electrostatic force as v approaches c. A single electron at a distance r from a cylinder of charge containing n_0 electrons/meter experiences an electrostatic force $F_E = (1/\epsilon_0)(n_0 e^2/2\pi r)$. If the cylinder moves with velocity v, its magnetic field is $B = \mu_0 v(n_0 e^2/2\pi r)$; and if the single electron moves with speed v in the same direction, it experiences a force $F_B = \mu_0 v^2(n_0 e^2/2\pi r)$, so that $F_B/F_E = v^2/c^2$. At 500 Mev the nearly perfect cancellation of electric and magnetic forces would permit a single-ring current of ~1000 times the 1 amp we intend to use. However, in the interaction region each electron of one ring finds the electric and magnetic forces of the other ring adding to give $2F_E$. We therefore approximate the problem of the interaction region forces by considering the effect on one electron of an oppositely-moving charge bunch. If the bunch is approximated as rectangular, 70-cm long, 0.5-cm wide, and h -cm high ($h \ll 1$ cm), containing charge corresponding to 1 amp of ring current, the E field at its surface is 6.5 kv/cm, and the effective field seen by the oppositely-moving electron is 13 kv/cm at the beam surface. It can be shown that this situation is on the edge of instability if the two beams are permitted to collide head-on.[22] If they cross at an angle θ, as is planned in this experiment, two effects should be considered: (i) Depending on azimuthal position in the bunch, each electron spends part of its time above and part below the opposing bunch. It therefore experiences a constant impulse once a revolution. This impulse is independent of vertical position of the electron within the bunch. It is equivalent to a magnetic field error, and produces a perturbed equilibrium orbit; the perturbation alters slightly the effective beam-crossing angle.

(ii) The fraction of time each electron spends above the opposing bunch has a small dependence on the vertical position of the single electron. This dependence makes the interaction region forces act as a thin lens, altering the vertical betatron wavelength. If the effect were large, the vertical oscillations could thus be driven onto a resonance.

(i) Perturbed equilibrium orbit.* All electrons receive a kick away from the one-electron orbit due to the interaction region forces. From Fig. G-1, one sees that the magnitude of this impulse goes from +V for electrons at the leading edge of the bunch to -V for electrons at the trailing edge. Since the displacement of an equilibrium orbit perturbed by a field error is opposite to the direction of the error at its azimuthal position (Fig. G-2), the effective beam crossing angle will be reduced by this effect. For an electron at the end of the bunch, the impulse due to the interaction region forces is $V = (13 \text{ kv/cm})(70 \text{ cm}) = 9 \times 10^5$ volts. The perturbed orbit will consist of ~0.85 of a vertical betatron oscillation (Fig. G-3). We describe the vertical oscillation by $A = A_0 \cos\omega_\beta t$; then at the interaction region point $\omega_\beta t = 0.85\,\pi$. Therefore, $A_B = A_0 \cos(0.85)\pi$ $= A_0 \cos 27^\circ = 0.89\, A_0$. At the interaction region position, $\dot{A} = \omega_\beta A_0 \sin\omega t$ $= \omega_\beta A_0 \sin 27^\circ = 0.45\, \omega_\beta A_0$. The impulse required to reverse the vertical velocity must cause a total change $2\dot{A} = 0.9\, \omega_\beta A_0$. In the regular guide field, the relation between impulse and angle is derived from

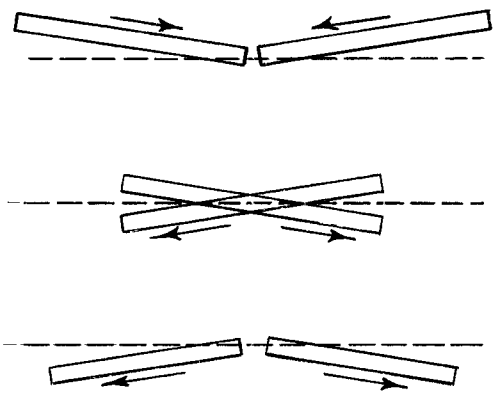

FIG. G-1

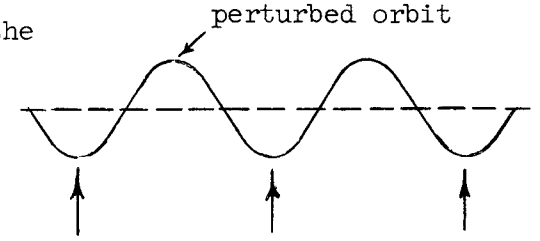

FIG. G-2

$$A' = A_0' \cos\omega_\beta t \; ; \qquad \dot{A}' = \omega_\beta A_0' \sin\omega t \; .$$

*The results of (i) were first obtained by P. Federbush.

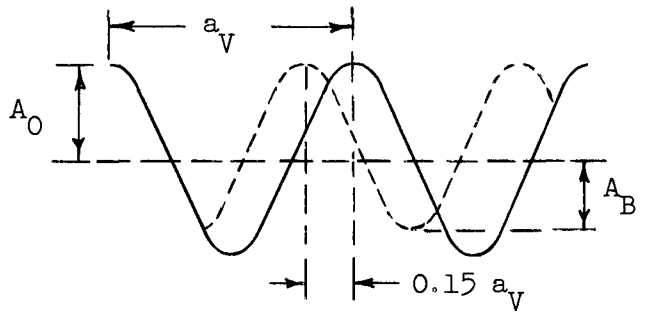

FIG. G-3

The impulse required to produce the maximum $\dot{A}'$ of an oscillation with magnitude A_0' is

$$V = \frac{15 \text{ kv}}{\text{cm}^2} \frac{a_V}{4} A_0' \overline{\sin\theta} \Big|_0^{\pi/2} = A_0' \, (2.5 \times 10^6) \text{ volts/cm} .$$

Therefore an impulse of 2.5×10^6 volts produces $\dot{A}' = \omega_\beta$, and the interaction region forces will produce

$$\Delta\dot{A} = \omega_\beta \frac{9 \times 10^5}{2.5 \times 10^6} \sim 0.36 \ \omega_\beta .$$

The amplitude A_0 of the orbit deviation due to the interaction region forces is then $A_0 = 0.36 \ \omega_\beta / 0.9 \ \omega_\beta = 0.4$ cm, for an electron at the end of the bunch. At the interaction region position, the deviation is $A_B = 0.89 \ A_0$ = 0.36 cm, and the resulting change in beam-crossing angle is $\Delta\theta = 2(\frac{0.36 \text{ cm}}{35 \text{ cm}})$ ~ 0.02 radian.

(ii) Alteration of vertical betatron wavelength. From Fig. G -4, the difference in distance traveled above and below the opposing bunch for an

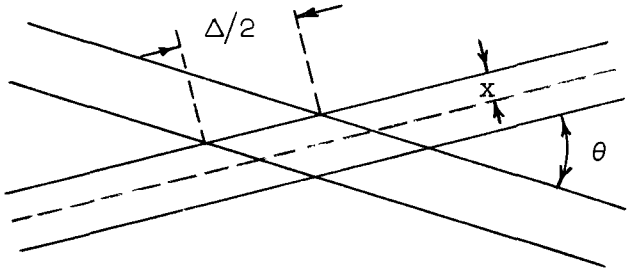

FIG. G-4

electron x cm from the equilibrium orbit is $2x/\theta$. The impulse picked up per revolution, due to a displacement x, is then

$$V = (13 \text{ kv/cm})(2x/\theta) = (26 \text{ kv}/\theta)x = (900 \text{ kv})x ,$$

for $\theta_{\text{effective}} = 0.03$ radian. The change in wavelength due to the thin lens of the interaction region forces can be found only by matrix multiplication; except for a factor of about unity, however, we can compare the interaction region forces to the guide field by noting that the vertical impulse given to an electron at a vertical displacement x is $V = (15 \text{ kv/cm})(x)\ell$ for ℓ cm of the guide field. The interaction region forces are therefore roughly equivalent to $\sim 900/15 = 60$ cm of the normal guide field, and alter the vertical betatron wavelength by $\sim 4\%$.

The exact calculation of oscillation amplitudes and wavelength alterations can be expected to differ from these approximate results by factors of ~1 to 2.

The longitudinal instability of two interpenetrating beams was studied by Sessler and Symon.[23] For the MURA intersecting beam model the energy spread in the beams was large enough to eliminate the instability. Comparison of the parameters of our storage rings with those of the MURA model indicates that our beams will also be stable against this effect.

APPENDIX H

CROSS SECTIONS, COUNTING RATES, AND BACKGROUND

A. Electron-Electron Scattering

The non-relativistic calculation of this process was first carried out by Mott.[24] Soon afterward Møller[25] performed the relativistic calculation for unpolarized electrons. It has been verified that electrons under the conditions of our experiment will be unpolarized, and that the radiative corrections probably will not alter Møller's calculation by more than 20%.

The Møller cross section in the center of mass is given by

$$\frac{d\sigma}{d\Omega} = r_0^2 \left(\frac{m_0 c^2}{E}\right)^2 \left(\frac{2}{\sin^2\theta} - \frac{1}{2}\right)^2 ,$$

where r_0 is the classical electron radius, E is the energy of one electron in the c.m. system, and we have assumed $E/m_0c^2 \gg 1$.

The interaction rate will depend on the length and width of the beam, but under the expected operating conditions should not depend on the beam height. The interaction rate R is given by

$$R = N_1 \rho_2 T_2 (2\sigma) f ,$$

where N_1 is the total number of particles in one bunch, ρ_2 is the density of the other bunch, T_2 its effective thickness, σ the cross section, and f is the circulation frequency in the storage rings. The factor of 2 in the equation comes from the motion of the target bunch.

Figure H-1 is a schematic of the crossing beams in the interaction region. Here h is the beam height and φ the crossing angle. In the

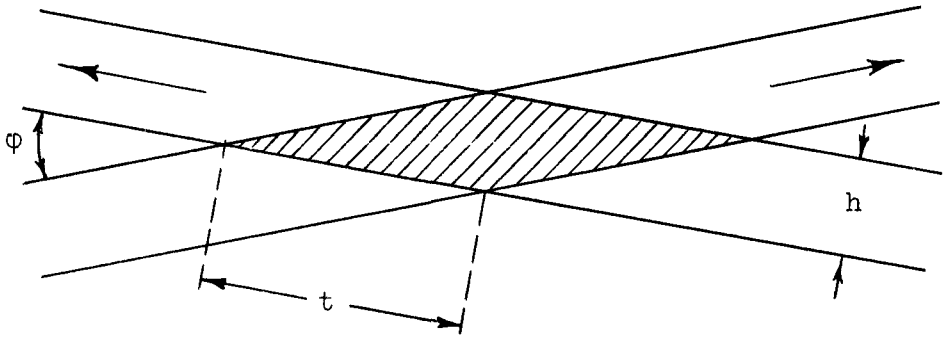

FIG. H-1.-- Configuration of the crossing beams in the interaction region.

approximation that $\varphi \ll 1$; that $h/\sin\varphi \ll \ell$, the bunch length; and that the two bunches are uniform and identical; then

$$R = (I/e)^2(2\sigma/\ell w f \varphi) ,$$

where I is the circulating current in one ring, e is the electronic charge, and w is the radial width of the bunch.

With $\varphi = 0.03$, $\ell = 70$ cm, $w = 0.5$ cm, and $I = 1$ amp,

$$R = 2.9 \times 10^{30}\ \sigma .$$

Table H-1 summarizes the expected counting rate.

B. Detection of Desired Events and Estimates of Background Counting Rates

1. Method of detection

The electron-electron scattering process has characteristics which permit it to be distinguished from a variety of possible background processes. First, the scattered electrons are in exact time coincidence and their directions of motion are almost exactly opposite; radiation accompanying the scattering disturbs the directional correlation slightly, but this is a higher-order process which can be taken into account. Second, the scattered electrons have the same energy (except for those scatterings accompanied by radiation) as the primary electrons, whereas electrons scattered

TABLE H-1. Summary of expected counting rates

Angle θ^*	Number of counters	$\Sigma\Omega_{\theta^*}$ (sterad)	$d\Phi(\theta^*)/d\Omega^*$ (cm^2/sterad)	Counts/sec
35°	8	0.18	2.4×10^{-30}	1.3
45°	12	0.27	0.96	0.75
55°	16	0.35	0.48	0.49
65°	20	0.44	0.30	0.38
75°	24	0.53	0.21	0.32
85°	28	0.62	0.18×10^{-30}	0.32
Totals	108	2.39	.....	3.6

by any stationary target will have energies that are considerably reduced by the recoil of the target particle or the occurrence of inelastic processes. Either or both of these characteristics can be used to advantage in picking out desired events. Because of the difficulty of achieving a large solid angle with an instrument capable of high energy resolution, it appears desirable to use the time and directional correlation as the primary means of identification of the e-e scattering events. An additional discrimination against background can be made by using detectors with some degree of energy selectivity.

The experiment has been designed to detect the e-e scattering events in many pairs of coincidence counters located on the surface of a sphere surrounding the interaction region. A possible arrangement of the detectors is shown in Figs. H-2 and H-3. Estimates of the signal and of the background counting rates will be based on the following parameters:

θ = angle of the detected particle relative to that of an incident particle;

L = distance from interaction region to detectors;

A = area of individual detectors;

τ = resolving time of coincidence circuit;

D = duty cycle of circulating beam
= (length of bunch)/(distance around orbit);

λ = decay constant of circulating beam; i.e., $I = I_0 e^{-\lambda t}$ where t is measured from the time injection stops;

I = circulating beam current;

f = circulation frequency of electrons in orbit;

n = number of electrons per bunch in one storage ring = I/fe ;

e = electronic charge = 1.6×10^{-19} coulomb;

p = pressure in storage rings in mm Hg.

2. Background due to scattering from residual gas in the neighborhood of the interaction region.

Because of the steep decrease of the scattering cross section with increase in θ, small-angle scattering events that can reach the detectors

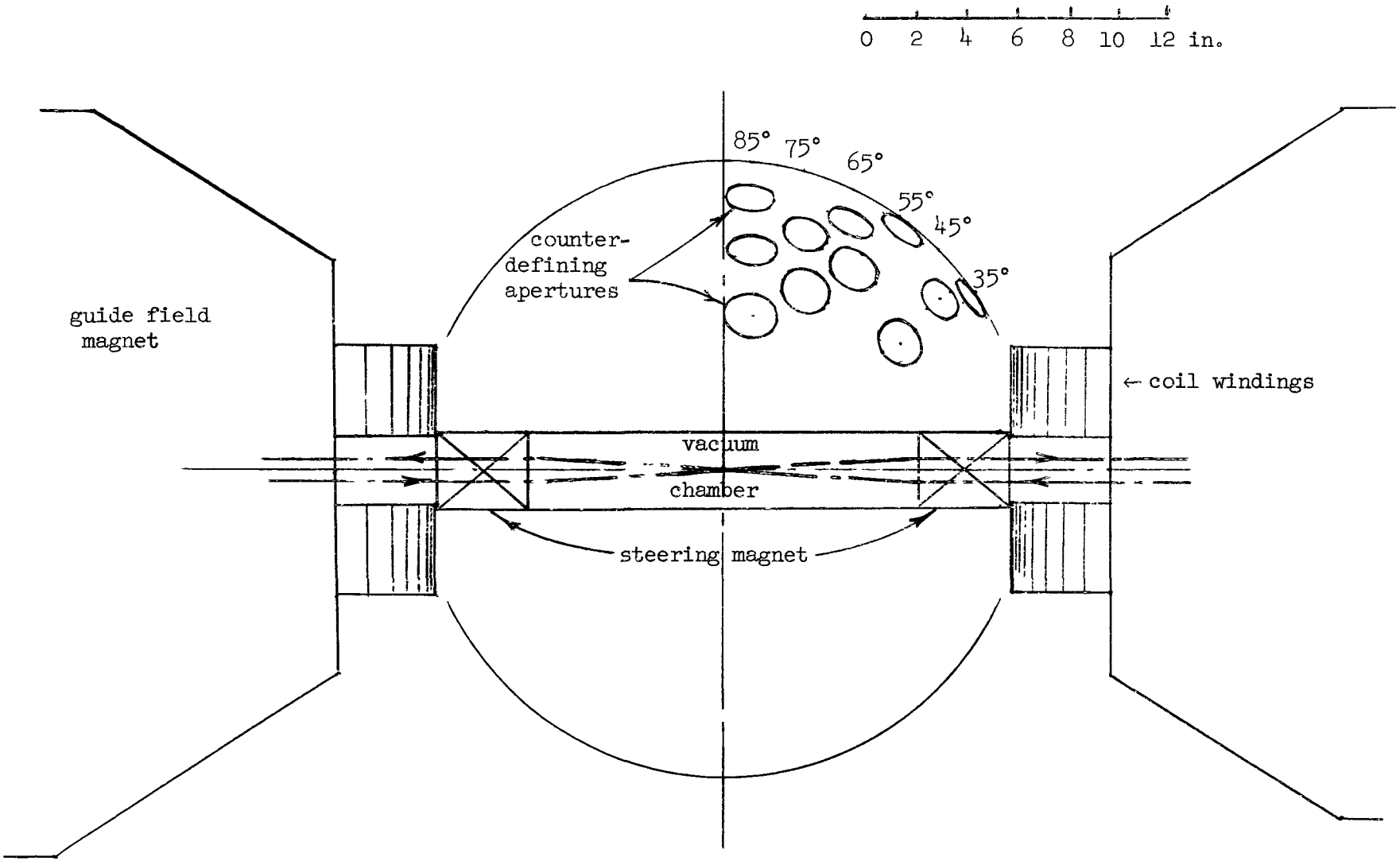

FIG. H-2.-- Side view of interaction region showing in one octant of the sphere the position of the counters.

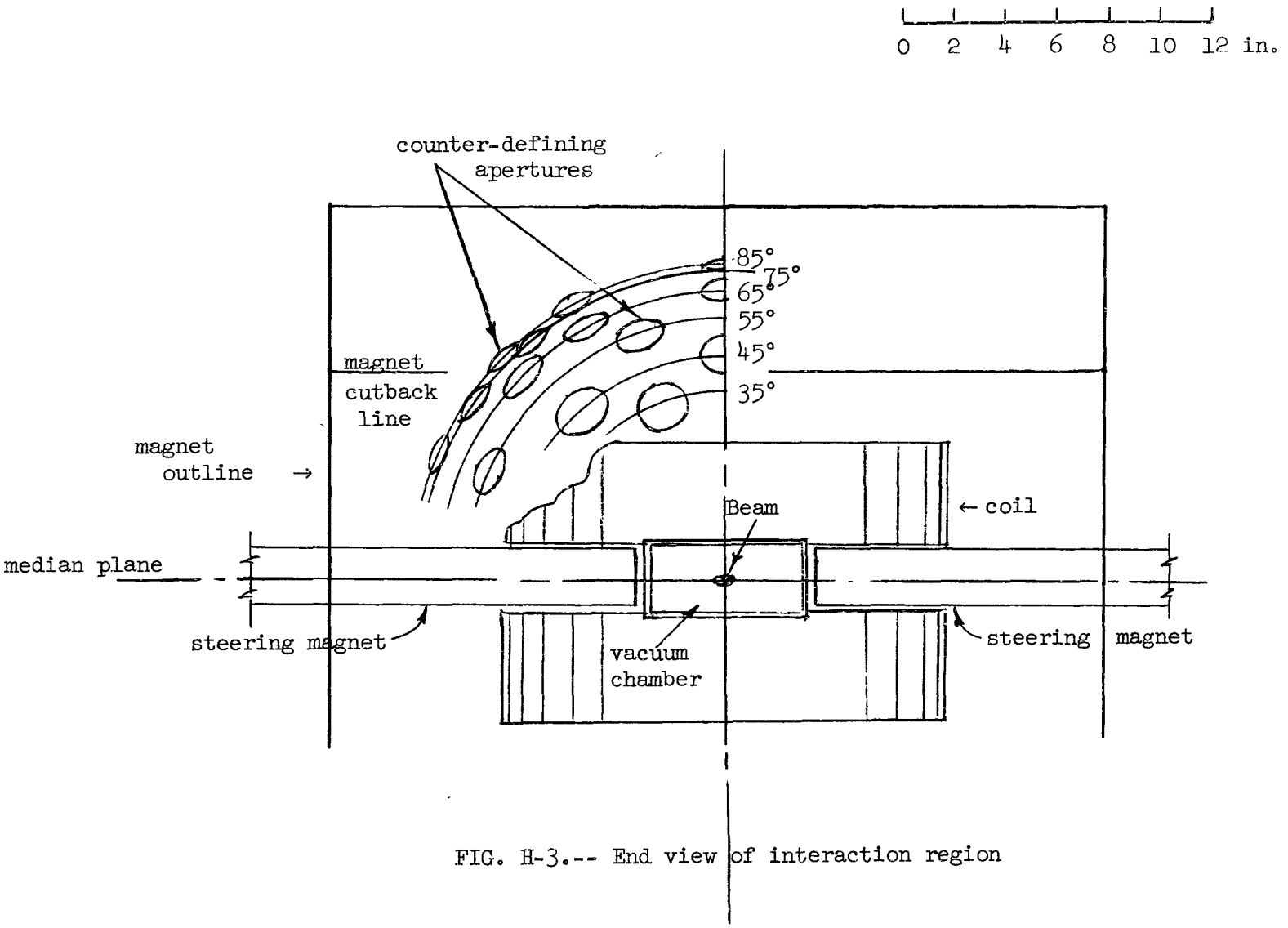

FIG. H-3.-- End view of interaction region

will be most serious. The geometry of the interaction region permits shielding to limit the smallest angle seen by the counters located at $\theta = 90°$ to more than $45°$ and the smallest angle seen by the counters located at $35°$ to $17°$. These limiting angles and an extreme effective target thickness of 50 cm will be used to calculate a maximum expected accidental rate. The elastic-scattering cross section for 500-Mev electrons on nitrogen atoms[27] are

$$(d\sigma/d\Omega)_{17°} = 5 \times 10^{-28} \text{ cm}^2 , \qquad (d\sigma/d\Omega)_{45°} = 10^{-32} \text{ cm}^2 .$$

At a gas pressure of p, in mm Hg, the number of target atoms in the effective target is

$$\frac{2 \times 6.02 \times 10^{23}}{22.4 \times 10^{3}} \times 50 \times \frac{p}{760} = (3.5 \times 10^{18})\, p .$$

The single counting rates due to beams circulating in both rings are approximately

$$R_{35°} = (3.5 \times 10^{18})\, p(I/e) \times (5 \times 10^{-28})[A/(2I)^2] ;$$

$$R_{90°} = (3.5 \times 10^{18}) p(2I/e) \times 10^{-32}(A/L^2) ,$$

in the $35°$ and $90°$ counters, respectively. The corresponding time average accidental coincidence counting rates are given by

$$C_{35°} = 2\tau(R_{35°})^2/D ,$$

$$C_{90°} = 2\tau(R_{90°})^2/D ,$$

where D is the duty cycle of the circulating beam. Numerical values of these rates are given in Table H-2 at the end of this Appendix.

3. Background due to mesons produced by the residual gas in the neighborhood of the interaction region.

To calculate the expected background due to the production of mesons we separate the calculation into two parts: (i) accidental coincidences due

to uncorrelated events; (ii) coincidences due to time-correlated events. In the second category we consider the production of two γ-rays from the decay of π^0's and the direct production of π-pairs.

In the calculations we make the following assumptions: (a) The yield of π^+-mesons from N^{14} by the bremsstrahlung beam has the same dependence on pion energy as in hydrogen, and its magnitude goes as $(Z/A)A^{\frac{2}{3}}$ (overestimate for N^{14}).[28] (b) The π^-/π^+ ratio on N is about unity.[29] (c) The π^0/π^+ ratio on N is about 2. (d) The angular distributions are isotropic (this is unknown but cannot make much difference). (e) The effective length of gas path is 50 cm. (f) Direct e-π production is determined by the Weizsäcker-Williams virtual photon spectrum, which we write approximately as

$$N_e(dk/k) \simeq (\alpha/\pi)(dk/k)\ \ln(E_0/k)\ ,$$

where E_0 is the electron energy and k is the photon energy. (g) The efficiency of the counters for detecting the γ-rays from π^0 decay is 10%.

The cross section for π^+ production by electrons is given by

$$\sigma_{\pi^+} = \frac{\alpha}{\pi}\int_{\text{threshold}}^{E_0} \sigma_{\pi^+}(k)\,\frac{dk}{k}\ln\frac{E_0}{k} \approx \frac{\alpha}{\pi}\ln\frac{E_0}{\bar{k}}\ \overline{\sigma_{\pi^+}(k)}\ \ln\frac{E_0}{150}\ ;$$

$$\overline{\sigma_{\pi^+}(k)} \approx 0.35 \times 10^{-27}\ , \quad \bar{k} \approx 300\ \text{Mev}\ ;$$

$$\sigma_{\pi^+} \approx (137\,\pi)^{-1} \times 0.35 \times 10^{-27} \times \ln 2 \times \ln 3.3 = 0.7 \times 10^{-30}\ ;$$

$$d\sigma_{\pi^+}/d\Omega = 0.6 \times 10^{-31}\ .$$

The average single counting rates are given by

$$N_{\pi^+} = \frac{d\sigma_{\pi^+}}{d\Omega}\,\frac{A}{L^2}\,\frac{2I}{e} \times (3.5 \times 10^{18})p\ .$$

The single rates due to π^+, π^-, and π^0 mesons (see Table H-2) are so low that the accidental coincidences are negligible under any possible operating conditions.

The coincidences due to correlated events are difficult to estimate, but we can calculate an "extreme" upper limit by assuming the γ-rays from π^0 decays and the charged pions from π-pairs are always directed exactly opposite. The effective cross section for π-pair production is only about 1% of that for π^0 production,[30] but since the efficiency of the counters for simultaneous detection of two γ-rays is only about 1%, the two processes will give about equal contributions to the counting rates. Since the number of π^0's produced is about twice the number of π^+'s the coincidence rate due to π^0's is

$$N_{\pi^0,\text{coincidence}} = 2 \frac{d\sigma_{\pi^+}}{d\Omega} \frac{A}{L^2} \frac{2I}{e}[(3.5 \times 10^{18})p] \times 10^{-2} ,$$

and an equal rate must be added for π-pair production. Numerical values are given in Table H-2.

4. Background from electron spill-out.

The background from electron spill-out is very difficult to estimate. Instead of trying to calculate this effect, we constructed a mock-up of the storage-ring magnets and used the Mark III electron beam to simulate the effects of the spill-out electrons. Since this background is expected to be worst in the 35° counters, the runs were done with counters set at that angle.

If we ask that the chance coincidence rate in the 35° counters be less than 1% of the true rate, we can compute the maximum tolerable singles rate:

$$R_c = R_s^2(\tau/D) \leqslant 3 \times 10^{-3} ,$$

where R_c is the chance rate, R_s is the singles rate, τ is the coincidence resolving time (assumed to be 5×10^{-9} sec), and D is the duty cycle of the circulating beam (assumed to be 1/16). Then,

$$R_s \leqslant 1.7 \times 10^2 \quad \text{counts/sec} .$$

The spill-out rate is

$$dn/dt = I\lambda/fe = 2.5 \times 10^8 \quad \text{electrons/sec} ,$$

where the beam lifetime $1/\lambda$ has been assumed to be 1000 sec. Without any beam scrapers in the storage rings, these electrons will spill out uniformly around the orbit. If we assume that only those electrons lost in the 10% of the orbit near the interaction region contribute to the background, we can tolerate a number of counts N per spill-out electron which is

$$N \leqslant 10\, R_s (dn/dt)^{-1} = 7 \times 10^{-6} .$$

The experimental test setup is shown in Fig. H-4. The steel plates

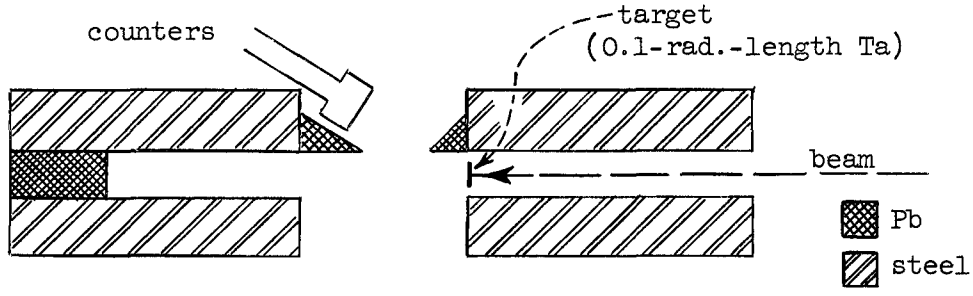

FIG. H-4. Schematic of beam spill-out background test setup.

were arranged to approximate the storage-ring magnets. The "gap" height and width were the same as those in the final storage-ring design. A 500-Mev electron beam from the Mark III accelerator was fired through the gap in the magnets, striking an 0.1-radiation-length target at the output of the first magnet, and an 8-in. thick lead block in the second magnet. The target was located at the worst possible position with respect to background in the 35° counters. (Since the vacuum chamber in the interaction region is larger than the magnet aperture, very few spill-out electrons will strike there.)

Both a Cerenkov counter and a liquid scintillator were used in the experiment. The counter biases were set to count minimum-ionizing particles passing completely through the counters. Under these conditions, 8×10^{-7} counts were recorded per incident electron. With the 0.1-radiation-length target removed, we found a yield of about 4×10^{-8} count per incident electron. Since we have been fairly pessimistic about the beam lifetime, we should not be seriously troubled by spill-out background.

5. Background due to cosmic rays

The coincidence counter pairs will probably be separated by a distance of about 60 cm, which requires a transit time of 2×10^{-9} sec for a particle with velocity c. Unless the resolving time is made less than this the main contribution of cosmic rays to the coincidence rate will come from single particles traversing the counter pairs. The expected counting rates, assuming a resolving time longer than the transit time between counter pairs, and a single particle sea-level flux of $10^{-2}\cos^2\lambda$ particles/cm^2-sterad-sec, are given by

$$10^{-2} \times (A^2/4L^2)\cos^2\lambda \ ,$$

where λ is the angle from zenith. The use of counter gates of 10^{-8} sec duration will reduce the rates by a factor of ~3. Values are given in Table H-2.

TABLE H-2. Signal and counting rates for one counter pair. The calculations assume A = 20 cm^2, L = 30 cm, D = 1/16, I = 1 amp, $\tau = 5 \times 10^{-9}$ sec.

Process	Singles (counts/sec)		Coincidence (counts/sec)		Comments
	$\theta = 35°$	$\theta = 90°$	$\theta = 35°$	$\theta = 90°$	
e-e scattering	325×10^{-3}	23×10^{-3}	325×10^{-3}	23×10^{-3}	
Gas scattering (elastic) $p = 10^{-7}$ mm	3.0	4.8×10^{-4}	negligible		Coincidence rate is propotional to p^2. Pressure should be $< 10^{-5}$ mm.
Meson production in gas $p = 10^{-7}$ mm	11×10^{-3}	11×10^{-3}	negligible		
Meson production--correlated events from π^o and π-pairs; $p = 10^{-7}$ mm	negligible		0.2×10^{-3}	0.2×10^{-3}	Grossly overestimated because of assumption that all secondary particles are oppositely directed.
Spillout; $\lambda = 10^{-3}$ sec^{-1}	< 170	$\ll 170$	$< 3 \times 10^{-3}$	$\ll 3 \times 10^{-3}$	From dummy experiment
Cosmic rays--counters in plane containing zenith	0.2	0.2	0.36×10^{-3}	1.1×10^{-3}	
Cosmic rays--averaged over all zenith angles	0.2	0.2	$\sim 0.18 \times 10^{-3}$	0.55×10^{-3}	10^{-8}-sec gates would reduce cosmic-ray counting rates a factor of ~3.

APPENDIX I

VACUUM SYSTEM AND TRAPPED-ION BEAM INSTABILITIES

The vacuum must be at least as good as 10^{-6} mm Hg if the storage lifetime is to be two minutes or more. There is no convenient intermediate range in vacuum design between a good conventional 10^{-6}-mm system and a nonorganic 10^{-9} to 10^{-10}-mm system, so the latter will be used. The vacuum chamber will be stainless steel, probably 3/16-in. thickness, with cooling pipes to remove the radiation heating. Standard Matterhorn gold-gasket joints, copper baffles, Alpert-type gauges, and an oil diffusion pump of small size will be needed. The entire double-ring system must be assembled, suspended on a frame, surrounded by a low-temperature oven, and baked out under vacuum at ~ 400°C.

In the beam injection process (Appendix A), the electrons need only pass through the magnetic channel once, but must make many traversals of the pulsed magnet after its field is turned off. The delay-line inflectors must therefore be located in the high-vacuum region. The inflectors contain only copper, ferrites, and ceramic condensers, which can stand bakeout temperatures.

Pickup electrodes for total circulating-beam monitoring will be needed in each ring. They must be more than 70-cm long if their signals are to be insensitive to the phase spread of the beams. If these electrodes are separated from the vacuum chamber walls by 3 mm, the capacity of each will be ~750 μμf. During initial tests, one should be able to detect a circulating current of a milliampere. The corresponding circulating charge (30 μμcoulomb) will produce a 40-mw signal at a 10-ohm impedance level.

Detection of beam position to the necessary accuracy can best be done with the help of the electrons' radiation. At 500 Mev, the radiation is sharply forward-peaked. A number of small windows are located at strategic points in the vacuum system, to view the circulating beams. For remote

operation, a system of fixed mirrors can present images of the beams for observation by telescope or TV camera. The view-ports must be protected from the small-angle x-radiation to prevent darkening of the glass.

Figure I-1 is a plan view of the vacuum chamber showing the location of windows, pulsed inflectors, pickup electrodes, and beam scrapers.

In the r-f sections, low-loss ceramic insulating pipes will separate the vacuum system from the accelerating cavities. The cavities can be split on a plane containing the beam axis, since no r-f currents need flow through such a plane.*

According to the Project Matterhorn vacuum system group, which has developed large ultrahigh-vacuum systems, one can expect an outgassing rate of 5×10^{-15} mm-liter/sec-cm^2 from well-baked stainless steel.[31] If one oil-diffusion pump baffled to 1 liter/sec is used, the equilibrium operating pressure should be 5×10^{-10} mm Hg in our 100,000 cm^2 system. A greater reserve capacity will be made available to take care of small leaks and helium permeation through glass and ceramics.

Trapped-ion instabilities——The ionization of residual gas by the circulating electron beam will lead to immediate beam loss unless the ions are removed promptly. With a 1-amp circulating beam and a 10^{-9} mm Hg operating pressure, the ion-pair formation rate will be $\sim 10^{12}$ ion pairs per second. Since there will be only $\sim 2 \times 10^{11}$ circulating electrons, the beam will make enough positive ions for neutralization of its space charge in less than a second. These ions can move only vertically in the presence of the magnetic field. If made with 2 ev of kinetic energy, they will move only 10^{-2} cm in one electron circulation time, and so cannot escape the trapping field of the beam. The average electric field of a 1-amp beam, measured at the beam surface and averaged over time, will be ~ 400 v/cm. During passage of the beam bunch, an ion initially at rest would acquire only 2 ev of energy. Possibly the net result of many traversals would be to cause gradual diffusion of the ions to the walls, but one could not design the experiment to depend on this effect.

---

*The split-cavity r-f geometry is being used by K. Robinson on the Cambridge Electron Accelerator.

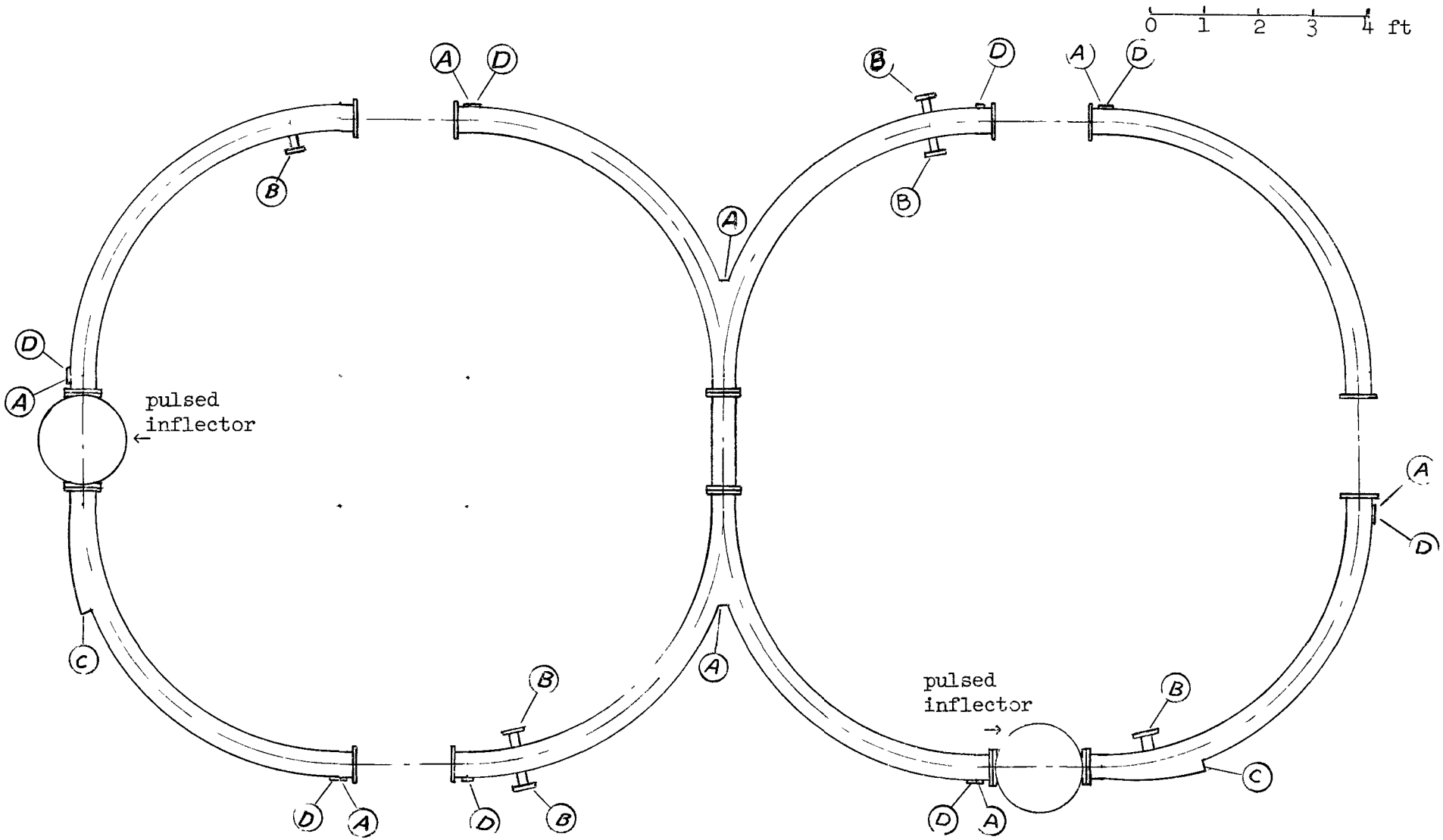

FIG. I-1.-- Layout of vacuum chamber

We can express the vertical focusing forces by an equivalent $\vec{E}$ field of the form $\vec{E} = -k\vec{x}$, where x is the displacement from equilibrium in cm: $\vec{F} = e(\vec{v}\times\vec{B}) = e\,\vec{E}_{equivalent}$. At 12 kilogauss, the main bending field is equivalent of 3.6×10^8 v/m. The vertical restoring forces are due to a field curvature such that the magnet pole tips would meet about two radii from the orbit. Thus,

$$E_{vert} = (-3.6 \times 10^8)x / (2.8 \times 10^2) = (-1.3 \times 10^6)x \quad (v/m)$$

$$= -13\,x \quad (kv/cm) .$$

If the beam is 10^{-2}-cm high, the focusing field at its surface will be $\sim$ 65 v/cm. With complete space-charge neutralization, this field would reach 500 v/cm, altering the vertical oscillation frequency by a large amount and causing rapid beam losses at the nearest resonance.*

By application of a clearing field greater than 400 v/cm, the positive ions can be removed quickly. If we use 1000 v/cm, the clearing time will be 0.5×10^{-6} sec, and no ion-trapping can occur. Insulated metal floor plates in the vacuum chamber, biased to $\sim$ 3 kv, will supply the clearing field. They will produce a useful side effect: the combination of an ionizing beam and a baked-out steel plate biased to several kv is an ion pump. With a 1-amp beam, the pumping speed due to this process should be $\sim$ 40 liters/sec, independent of pressure, and may produce even higher vacua than can be made by the oil pumps.

---

*Beam losses apparently due to this effect have been observed and identified in an electron model accelerator by members of the MURA group; cf. reference 32.

APPENDIX J

RADIOFREQUENCY POWER

The radiation losses are 4 kev/turn (incoherent) plus a small coherent loss estimated at less than 0.1 kev/turn. The minimum required r-f voltage, for a 100-sec beam lifetime, is 12 kv; 20 kv will be made available to allow for errors of approximation in the calculations. The dependence of beam lifetime on r-f voltage is very steep, and the loss time against quantum fluctuations at 20 kv should be at least many days.

One straight section in each storage ring will include lengths of low-loss ceramic pipe. These will be enclosed by split r-f cavities running in air at 25.4 Mc, powered by single-tetrode amplifiers. For a copper r-f cavity of shape and size needed to fit a storage-ring straight section and resonate at 25.4 Mc, the r-f resistance and Q have been calculated. The Q should be more than 5000, and the shunt impedance about 10^5 ohms. The total r-f power needed for the two cavities should be 12-20 kw; the required tubes are a small standard type in current production.

It will be convenient to provide an adjustable phase shift between the two cavities. The background counting rate due to the residual gas can then be approximately checked without altering the circulating electron current, by dephasing the circulating beams until they no longer collide.

REFERENCES

1. R. Hofstadter, Revs. Modern Phys. 28, 214 (1956), and references contained therein.

2. R. P. Feynman and G. Speisman, Phys. Rev. 94, 500 (1954).

3. Berestetskii, Krokhin and Khlebnilov, Soviet Phys. JETP 3, 761 (1956).

4. B. Richter, Phys. Rev. Letters 1, 114 (1958).

5. S. D. Drell, Ann. Phys. 4, 75 (1958).

6. G. K. O'Neill, Phys. Rev. 102, 590 (1956), and quoted references.

7. -----, Proceedings of the CERN Symposium on High Energy Accelerators and Pion Physics (Geneva, CERN, 1956), vol. 1, p. 64.

8. V. A. Petuhkov, J. Exp. Theor. Phys. (USSR) 32, 379 (1957).

9. T. Ohkawa, "A scaled radial sector FFAG for intersecting beams," MURA report TO-6, 9 July 1956 (unpublished), and succeeding reports.

10. G. K. O'Neill and J. A. Ball, "An experiment on the structure of the electron," Princeton University Palmer Physical Laboratory report, 18 July 1957 (unpublished).

11. R. F. Christy, "Synchrotron beam loss due to quantum fluctuations in radiation," California Institute of Technology (unpublished).

12. G. K. O'Neill and V. Korenman, "The delay-line inflector," Princeton University Accelerator Project internal report no. GKO'N-10, VK-3, 18 December 1957 (unpublished).

13. D. J. Grove, "Some observations on the behavior of copper traps and UHV systems of moderate size," Princeton University Project Matterhorn Technical Memorandum no 40, 15 February 1957 (unpublished).

14. W. C. Barber, "Injection magnets," High-Energy Physics Laboratory report no. HEPL-163, (16K/WCB-1), 20 March 1959 (unpublished).

15. M. Sands, Phys. Rev. 97, 470 (1955).

16. A. A. Sokolov and I. M. Ternov, J. Exp. Theor. Phys. (USSR) 24, 249 (1953).

17. A. A. Kolomenskii and A. N. Lebedev, J. Exp. Theor. Phys. (USSR) 3, 130 (1956).

18. K. Robinson and D. M. Ritson, Cambridge Accelerator Project report no. CEA-14, 1955 (unpublished).

19. J. A. Ball, "Scattering from residual gas," Appendix 3 of reference 10.

20. F. S. Crawford, Jr., "Destruction of stored cyclotron beam by Coulomb scattering," University of California Radiation Laboratory report no. UCRL-3464 (unpublished).

21. E. Fermi, Nuclear Physics (Chicago, University of Chicago Press, 1950), p. 46.

22. P. Federbush, "Betatron oscillations generated in the interaction region of an electron storage ring" (unpublished).

23. A. M. Sessler and K. R. Symon, Bull. Am. Phys. Soc., Ser. II, 4, 55 (1959).

24. N. F. Mott, Proc. Roy. Soc. (London) 126, 259 (1930).

25. C. Møller, Ann. Physik 5F14, 563 (1932).

26. F. J. Dyson (private communication).

27. R. Hofstadter, Ann. Rev. Nuc. Sci. 7, 231 (1957).

28. Williams, Crowe and Friedman, Phys. Rev. 105, 1840 (1957).

29. R. M. Littauer and D. Walker, Phys. Rev. 86, 838 (1952).

30. R. M. Friedman and K. M. Crowe, Phys. Rev. 105, 1369 (1957).

31. D. J. Grove, reference 13.

32. F. E. Mills and D. S. Roiseland, Bull. Am. Phys. Soc., Ser. II, 3, 168 (1958).